Computations of Object Motion in the Visual Cortex of the Ferret

Von der Medizinischen Fakultät
der Rheinisch-Westfälischen Technischen Hochschule Aachen
zur Erlangung des akademischen Grades
einer Doktorin der Medizin
genehmigte Dissertation

vorgelegt von
Sarah Wehner
aus
Aachen

Berichter: Frau Universitätsprofessorin
Dr. med Katrin Amunts

Herr Universitätsprofessor
Dr. med. Karl Zilles

Tag der mündlichen Prüfung: 23. November 2009
Diese Dissertation ist auf den Internetseiten der Hochschulbibliothek online verfügbar.

Contents

1 Introduction

1.1 Entering

It is of fundamental importance to perceive and process motion of objects in our environment and even predict their future position along a motion trajectory. A stimulus in the visual field is first mapped on the retina. Here the upper visual hemifield (elevations above zero degrees) is mapped on the inferior half of the retina. The lower visual hemifield (elevations below zero degrees) is mapped on the superior half of the retina (Schmidt et al., 2000; Palmer, 2002). Then the retinal image is processed by the lateral geniculate nucleus (LGN) of the thalamus, the primary visual cortex and finally by higher order visual areas (Schmidt et al., 2000; Palmer, 2002; McIlwain, 1996). The retinotopic organization of the mapping of the visual field is maintained along early areas of visual computation and in most of the parietal visual areas (McIlwain, 1996). When watching a moving stimulus with the head and eye fixed, the cortical representation of the stimulus can be expected to move accordingly, in retinotopic coordinates over the cortex. Although this statement seems consequential it has not been tested experimentally previously. To investigate the cortical processing of continuously moving visual stimuli a technique is required that allows for high resolution in both spatial and temporal domains. Furthermore, an animal model is required that has a well-developed and well-understood visual system. With Voltage Sensitive Dye Imaging and multi unit recordings the computation of moving objects was experimentally investigated in the visual cortex of the ferret.

1.2 Anatomy of the visual system

As a first step of vision, the photoreceptor cells of the retina collect photons as sensory input from the environment. Here, for each eye, the lateral visual hemifield (lateral to the vertical meridian) is mapped to the nasal part of the retina. The medial visual hemifield (medial to the vertical meridian) is mapped to the temporal part of the retina. The upper visual hemifield (above the horizontal meridian) is mapped to the inferior half of the retina; the lower visual hemifield (below the horizontal meridian) is mapped to the superior half of the retina. The processed signal is forwarded via bipolar cells to the neurons of the optic nerve (the retinal ganglion cells) (Figure 1). The axons of these neurons exit the retina and traverse as optic nerve to the optic chiasm. For mammals with frontal placement of the eyes, the fibres originating from the nasal parts of the retinas cross to the contralateral side of the brain, fibres originating from the temporal parts of both retinas remain on the ipsilateral side. This results in images from the right visual hemifield being processed in the left half of the brain and images from the left visual hemifield being processed in the right half of the brain. From the optic chiasm the optic tract traverses to the lateral geniculate nucleus (LGN) of the thalamus. From the LGN the neurons traverse as the optic radiation to the primary visual Cortex (V1), or

Brodmann's area 17, in the occipital lobe. Here, the retinal representation of the computed image is mapped to the cortex. In V1 the first steps of cortical visual processing are performed. Still, the retinotopic organization is maintained and ipsi- and contralateral eye inputs mostly remain separated.

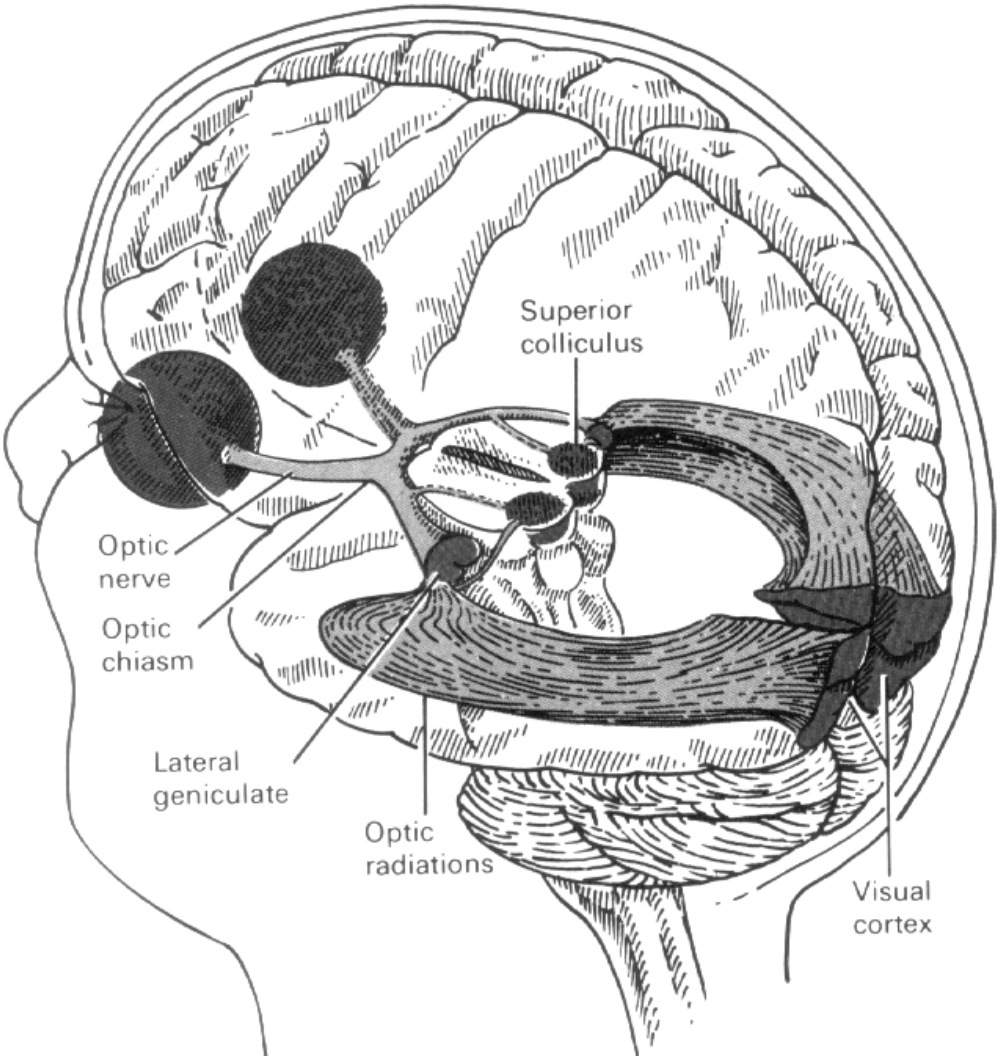

Figure 1: Different stages of visual processing from the eye via the optic nerve, optic tract and optic radiation to the primary visual cortex in a human brain. Copied from Palmer, S. "Vision Science, Photons to phenomenology", (2002).

The center of visual field has a greater cortical representation than the periphery (Figure 2). Neurons in the center representation have small receptive fields. Thus, they receive inputs from small parts of the retina. The receptive field size of neurons increases with their distance from the foveal representation. This allows the center of visual field to be represented in great detail while the periphery is represented in less detail.

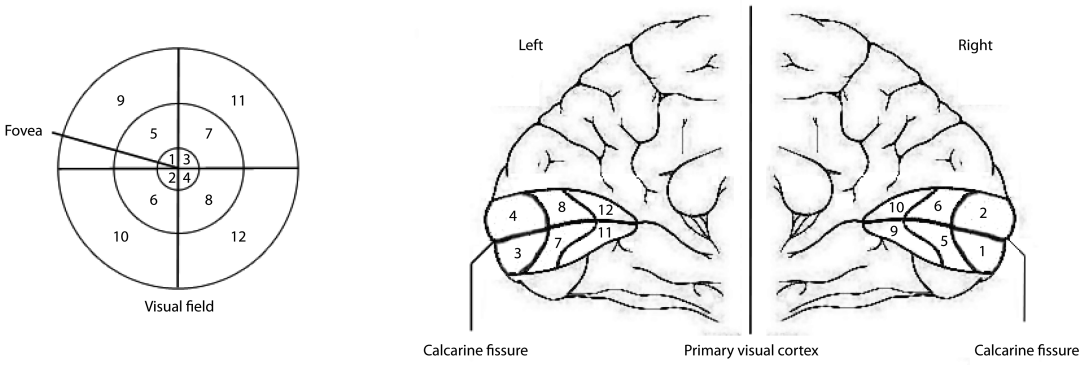

Figure 2: Mapping of the visual hemifields to the hemispheres of the primary visual cortex in a human brain. Each hemisphere of the brain receives input from the contralateral visual hemifield. The images are traversed to the cortex in an "upside down" position. Note the different size of representation for the center of visual field as opposed to the periphery in the primary visual cortex.

From area 17 in the occipital lobe visual signals are transmitted as feed forward action potentials to higher order visual areas, i.e. Brodmann's areas 18, 19 and 21 (or V2-V6 in the monkey brain) as well as to higher order visual areas in the temporal and parietal lobe (Figure 3).

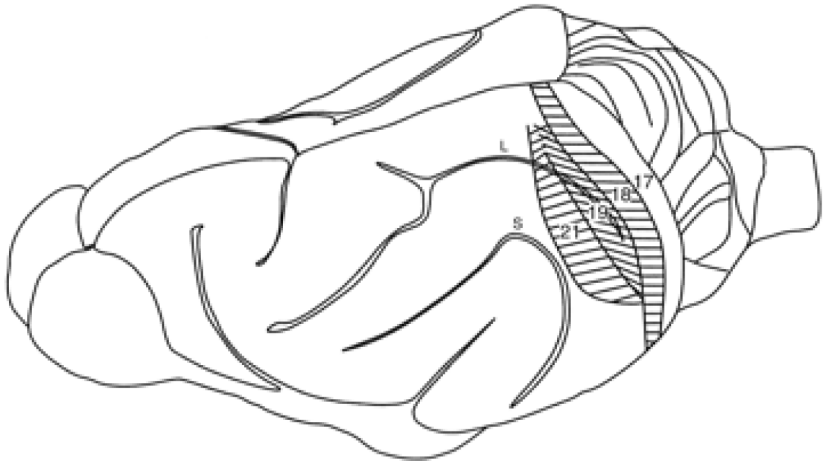

Figure 3: A ferret brain with areas 17, 18, 19 and 21 marked in the occipital lobe. L shows the lateral sulcus, S the suprasylvisan sulcus. Copied from Innocenti et al., 2002 "Architecture and Callosal Connections of Visual Areas 17, 18, 19 and 21 in the Ferret (Mustela Putorius)"

The feed-forward action potentials arriving from the LGN in area 17 travel towards higher order areas in two processing streams: The ventral and the dorsal stream (Ungerleider et al., 1983; Ungerleider & Haxby, 1994; Gattass et al., 1990). The ventral stream originates in area 17, passes through the occipital visual areas and targets areas in the temporal lobe. In the ferret, this stream travels through areas 18, 19 and 21, laterally and posterior to the suprasylvian sulcus. The temporal stream terminates in areas 20a, 20b and PS (Posterior suprasylvian). These temporal areas show similarities to the areas with the same labels in the cat (Manger et al., 2004) as

well as to monkey areas TF, TH and TG (Payne, 1993). The ventral stream is called the "what pathway" and is involved in the processing of non-metric properties, such as shape, colour and texture of an object. It is associated with form recognition and object representation. The dorsal stream travels from area 17 through areas 18, 19 and 21 to the parietal lobe. In the ferret it targets the Posterior Suprasylvian area (PSS, similar to areas MT and MST in the monkey (Zeki, 1974; Philipp et al., 2006) and PMLS in the cat (Philipp et al., 2006; Cantone et al., 2006)), the Caudal Posterior Parietal area (PPc, similar to monkey area 7, Manger et al., 2002) and the Rostral Posterior Parietal area (PPr, similar to monkey area 5, Manger at al., 2002). This stream is called the "Where pathway". It is involved in the processing of metric properties of visual stimuli such as size, depth, motion computation and object location. Neurons representing the fovea in area 17 (V1) have the smallest receptive fields. The receptive field size increases with eccentricity within one area and with every step of cortical processing in subsequent and thus higher order areas (Manger et al., 2002). It has been known for some time that the processing of visual information is not performed in a strict feed-forward order from lower towards higher order visual areas. As a top-down mechanism feedback travels from higher to lower order visual areas providing the base for bidirectional information processing (Bullier, 2001; Sincich & Horton, 2005, Roland et al., 2006). In addition a lateral spreading depolarization activates neurons within one cortical area (Grinvald et al., 1994; Roland et al., 2006). This results in computational circuits rather than a strict hierarchical arrangement of visual areas. As a part of the neocortex, the visual cortex is organized in six layers. Layer IV is called granular lamina due to its granular appearance in histological sections. Layers I to III are called the supragranular laminae, layers V and VI the infragranular laminae. Feed forward connections originate in the supragranular laminae (or the LGN) and terminate in lamina IV (Hendrickson et al., 1978; Diamond et al., 1985; Sincich & Horton, 2005). Feedback and lateral anatomical connections originate and terminate outside the granular laminae (Felleman & van Essen, 1991; Eriksson & Roland, 2006).

1.3 Current state of research

1.3.1 The visual cortex of the ferret

As Manger et al. (2002) have shown, in the visual cortex of the ferret, the vertical meridian (zero degree azimuth) is mapped at the border between areas 17 and 18. Image representations are mirrored at the 17/18 border, i.e. area 18 shows a mirror reversal of area 17. A second representation of the vertical meridian is mapped as the border between areas 19 and 21. Area 21 shows a mirror reversal of area 19. Receptive field size increases with azimuths, i.e. distance to the vertical meridian. The horizontal meridian is represented continuously throughout areas 17, 18, 19 and 21. Elevations above zero degrees are mapped lateral; elevations below zero degrees are mapped medial to the horizontal meridian. Cells at or close to

the horizontal meridian have small receptive fields; at more medial or more lateral positions receptive field size increases. The first ten degrees of elevation above and below the horizontal meridian occupy one third of the medio-lateral extension of the visual cortex in areas 17 and 18. The rest of the visual field is mapped to the remaining two thirds above and below. The center of visual field is mapped at the crossing of the mapping of the vertical and horizontal meridian. Due to the dual representation of the vertical meridian there are two foveal representation sites, one at the 17/18 border and one at the 19/21 border. In area 21 the horizontal meridian splits up resulting in a more complicated organization of representation (Manger et al., 2002) (Figure 4). Central positions of the visual field are mapped along the vertical meridian at the 17/18 and 19/21 borders and along the horizontal meridian throughout areas 17, 18 and 19. Peripheral positions are mapped to the posterior border of area 17, to the border between areas 18 and 19 and to the anterior border of area 21 (azimuths) and at the medial and lateral parts of the areas (elevations). Receptive field size increases from the 17/18 border across areas 18, 19 and 21 (Manger et al., 2002).

Given this retinotopic organization of the early visual areas, a stimulus presented to a ferret in the center of field of view can be expected to be mapped to two positions on the visual cortex: to the crossing of the vertical and horizontal meridian at the 17/18 and at the 19/21 border (Roland et al., 2006). Stimuli in the periphery of the visual field will result in representations mapped at the corresponding positions along the azimuths and elevations mapped on the cortical surface. A moving stimulus presented to a fixed eye will create an image moving across the retina. In analogy to the image positions on the retina, the stimulus representation will move along the corresponding retinotopic positions on the cortical surface. A stimulus appearing in the center of field of view and then moving upwards will be represented at the crossing of the horizontal and vertical meridian in areas 17/18 and 19/21 and then move laterally along the vertical meridian. A stimulus appearing in the center of visual field and moving downwards will be represented at the same initial position and then move medially along the vertical meridian.

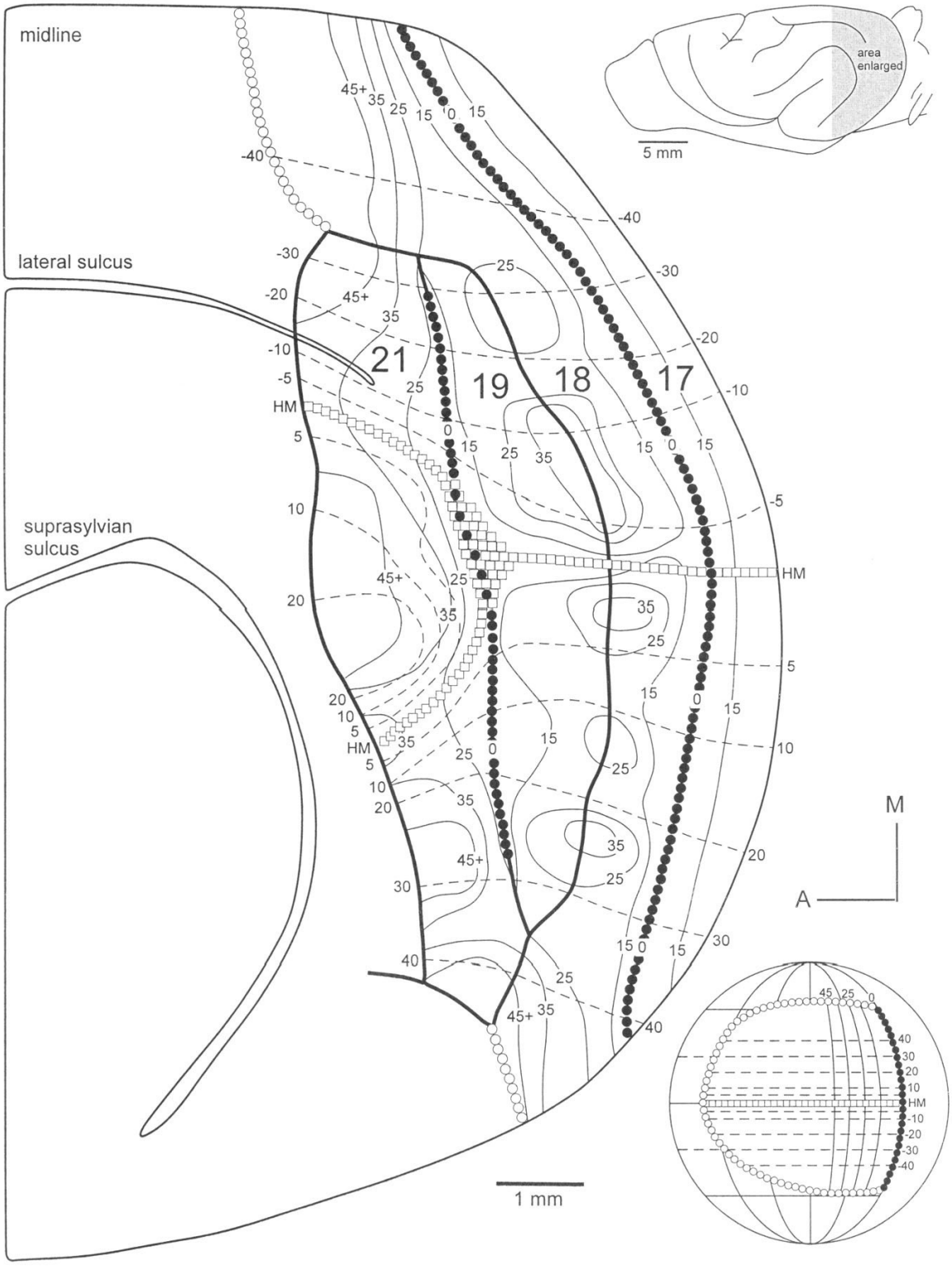

Figure 4: Areas 17, 18, 19 and 21 of the ferret brain. The relevant areas are enlarged as shown in the figurine in the right upper corner. Black dotted lines show the two cortical representations of the vertical meridian. It is situated at the 17/18 and the 19/21 borders. Squared lines show the representation of the horizontal meridian. Azimuth and elevation lines are shown and marked with degrees. A: anterior, M: medial. Copied from Manger et al., 2002 "The Representation of the Visual Field in Three Extrastriate Areas of the Ferret (Mustela Putorius) and the Relationship of Retinotopy and Field Boundaries to Callosal Connectivity"

1.3.2 Investigation of cortical activity

During the past decades neuronal activity in the cerebral cortex has been studied with different techniques. With recording electrodes placed at distinct cortical sites action potentials of single or multiple neurons and local field potentials were detected. Spontaneous and evoked cortical activity was investigated and temporally correlated to sensory input (Mountcastle, 1957; Hubel & Wiesel, 1959, 1962; Arieli et al., 1995; Roland, 2002). However, the method of recording action potentials with electrodes has restrictions in the investigation of neuronal activity: One is the limited spatial potency. Cellular activity can only be investigated close to the recording site of the electrode. Since the activity of each neuron is influenced by other neurons forming a network across cortical areas (Roland, 2002, Grinvald & Hildesheim, 2004) it was mandatory to record the activity of large cell populations. However, even with arrays of multiple electrodes one can only record activity at distinct points of cortex (Shoham et al., 1999). The anatomical configuration of the cortex made it difficult to lower electrodes into the brain at certain positions, e.g. around blood vessels or inside sulci. The high impedance electrodes needed to record action potentials only allowed measurement of suprathreshold activity, i.e. action potentials of single or multiple neurons (Schmidt et al., 2000; McIlwain, 1996). Since it is the sub-threshold activity, i.e. changes in membrane potential that determine neuronal computations (Grinvald & Hildesheim, 2004), a lot of information about the ongoing activity was lost. Other techniques with high temporal resolution like electroencephalography (EEG) and magneto encephalography (MEG) also had poor spatial resolution (Shoham et al., 1999; Grinvald & Hildesheim, 2004). Furthermore, the relation between these signals and membrane potentials and action potentials is very indirect, leading to ambiguous information about neuronal activity (Arieli at al., 1995; Shoham et al., 1999). Techniques with high spatial resolution like functional magnetic resonance imaging (fMRI), 2-deoxiglucose-mapping (2-DG), positron emission tomography (PET) or optical imaging of intrinsic signals (OIIS) showed poor temporal resolution (Shoham et al., 1999; Grinvald & Hildesheim, 2004). Summarizing, none of the named techniques provided both unambiguous information and sufficient spatial and temporal resolution.

1.3.3 New methods

To investigate the cortical processing of stimuli a technique is required that allows the detection of network activity across cortical areas with high resolution in both temporal and spatial domains (Roland, 2002). Voltage Sensitive Dye Imaging (VSDI) fulfils these requirements. With a micrometer spatial and a sub millisecond temporal resolution network dynamics can be recorded in several cortical areas simultaneously (Grinvald & Hildesheim, 2004). Voltage Sensitive Dyes reveal supra- as well as sub-threshold cortical activity (Slovin et al., 2002; Grinvald & Hildesheim, 2004) rather than being restricted to the detection of action potentials. Cortical ac-

tivity can be detected in both anaesthetized and behaving animals (Shoham et al., 1999; Slovin et al., 2002) allowing for various study designs. The only limitations are the spatial resolution of the imaging system and the signal to noise ratio (Shoham et al., 1999). The cortex can be stained with Voltage Sensitive Dyes. The dye molecules bind to the external part of membranes in the cortical tissue (Arieli et al., 1995; Grinvald & Hildesheim, 2004) (Figure 5). When the membrane potential of a stained neuron changes, the dye responds with a linear change in spectral fluorescence (Arieli et al., 1995). This change can be detected with a photodiode array camera (see methods section for setup details). The dye signal increase is proportional to both the extension of the area (i.e. the amount of stained membranes) imaged by a given photo detector and the level of change in membrane potential (Cohen et al., 1974; Grinvald & Hildesheim, 2004). The VSD binds to all cortical cell membranes, therefore signals from all cortical cell types will be acquired, i.e. axons, cell-bodies, dendrites and glia. Since dendrites occupy a much greater deal of cortical space than axons and cell somata (Grinvald & Hildesheim, 2004) the VSD-Signal is mostly a dendrite signal, displaying sub-threshold activity of large networks of cells (Slovin et al., 2002; Grinvald & Hildesheim, 2004).

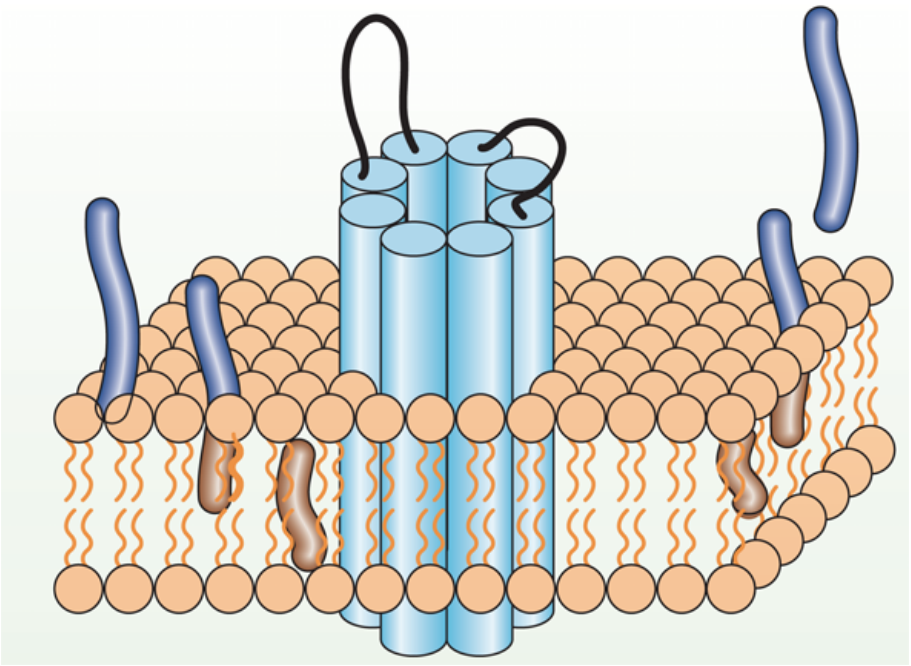

Figure 5: A model of a cell membrane (yellow) with an ion channel (light blue). Several dye molecules (dark blue) are binding to the membrane. Copied from Grinvald & Hildesheim, 2004 "VSDI A New Era in Functional Imaging of Cortical Dynamics"

The first recordings with Voltage Sensitive Dyes were made by Tasaki and collaborators (Tasaki et al., 1968) and by Cohen and colleagues (Cohen et al., 1974). It was shown that Voltage Sensitive Dyes display changes in membrane potential rather than current (Cohen et al., 1974). This is similar to intracellular recordings of single cells with sharp electrodes. During the past decades multiple different dyes were

synthesized with improving penetration properties and signal to noise ratio as well as decreasing photodynamic tissue damage (Waggoner et al., 1977; Waggoner, 1979; Grinvald et al., 1982; Shoham et al., 1999). In the past years the visual cortex of monkeys and cats has been investigated (Arieli et al., 1995; Shoham et al., 1999; Slovin et al., 2002; Grinvald & Hildesheim, 2004; Jancke et al., 2004), providing sophisticated information about ongoing activity. Roland and coworkers (2006) have established VSDI in the visual cortex of the ferret and have investigated stationary and apparent motion stimuli. Since the VSD signal is mostly a dendrite signal it is necessary to combine Voltage Sensitive Dye Imaging with electrophysiological recordings. Spiking activity of neurons in a given area can then be correlated to the network membrane potential revealed by the dye. Combining these two methods processes in the neocortex can be investigated at very high spatial and temporal resolution with a maximum outcome of information.

1.4 Aim of this study

To study visual computation of moving stimuli VSDI and multi unit activity recording are the most feasible methods. By investigating spiking activity and changes in population membrane potential detailed information about activity in large cortical areas can be revealed. Thus, the computation of moving stimuli can be explored along subsequent representation sites of the moving stimulus, not only in the primary visual cortex but also in higher order visual areas. Furthermore, activity can be investigated over a time range long enough to allow for a stimulus to change its position along a motion trajectory. As an animal model the ferret (Mustela putorius) was chosen. It has a relatively complex brain with a higher amount of convolutions compared to other small animals, e.g. rodents. The ferret brain has a more sophisticated visual system and resembles the human brain more closely. However, the ferret is smaller and easier to handle than cats or monkeys. It has been used as a model in numerous previous studies investigating the visual cortex. Therefore a lot of information on anatomy, experimental procedures and study design is available. Since it has not been tested experimentally before, this thesis has the aim to show the motion of a cortical stimulus representation site according with the retinal image in the visual cortex of the ferret.

2 Materials and methods

2.1 Animals

All animal experiments were approved by the Stockholm regional Ethics Committee and performed according to European Community guidelines for the care and use of animals in scientific experiments. The study was done on six adult female ferrets (Mustela putorius) between eight and eighteen months of age and 700 and 1000g of weight. All animals were purchased from a local authorized breeder. The animals were housed in the animal facilities of Karolinska Institutet, Stockholm, Sweden and supervised by animal keepers and veterinarians. They were kept in groups of up to six animals in big rooms (12.5m^3) with environmental enrichment. Temperature was kept at 22°C; ventilation and humidity were not controlled. The rooms had a 12-hour light-and-dark cycle (lights on at 07:00 am). The animals had access to food (Whiskas cat food, 200g/animal/day and Royal canin dry food pellets, 1.5dl/six ferrets, twice a week) and water ad libitum. All experiments were performed at the Department of Neuroscience of the Karolinska Institutet, Stockholm, Sweden.

Table 1: List of animals used in this study with corresponding ID-Numbers, weight and date of the experiment.

Animal	*ID-Number*	*Weight (g)*	*Date of Experiment*
1	334	682	2006-05-19
2	337	992	2006-05-22
3	340	824	2006-06-05
4	346	874	2006-06-28
5	356	868	2006-07-11
6	357	855	2006-07-13

2.2 Chemicals and equipment

Table 2: List of chemicals and equipment used during the experiments (a).

Product	*Manufacturer, Components*
Initial anaesthesia	Medetomidinhydrochloride (DOMITOR®VET), 1mg/ml, Orion Pharma, Orion Corporation, Espoo, England Ketaminhydrochloride (Ketalar®), 50mg/ml, Pfitzer AB, Täby, Sweden Atropine, 0.5mg/ml, NM Pharma AB, Stockholm, Sweden
Corticosteroids	Dexamethason (Vorenvet®vet), 1mg/ml, Boehringer Ingelheim, Ingelheim/Rhein, Germany
Paralysis	Pancuroniumbromide (Pavulon®), 2mg/ml, N.V. Organon, Oss, The Netherlands, Initial dose 0.5mg kg^{-1}, then 0.6 mg kg^{-1} h^{-1} Perfusor Bender & Hobein, Zurich, Switzerland
Eye drops	Atropine, 1%, Alcon, Alcon-Couvreur, Puurs, Belgium Phenylephrine, 5%, Novopharma AG, Seinhausen, Germany

Table 3: List of chemicals and equipment used during the experiments (b).

ACSF (ph 7.4)	100ml distilled water 26mg $CaCl_2$, Sigma-Aldrich Chemie GmbH, Steinheim, Germany 20mg $MgCl_2$, Sigma-Aldrich Chemie GmbH, Steinheim, Germany 780mg NaCl, Merck KGaA, Darmstadt, Germany 37mg KCl, Sigma-Aldrich Chemie GmbH, Steinheim, Germany 119mg HEPES Buffer, Sigma-Aldrich Chemie GmbH, Steinheim, Germany
VSD	RH-1838, 0.8mg/1.5ml ACSF, Optical Imaging, Rehovot, Israel
Contact lenses	Nordiska lins, Göteborg, Sweden
Sacrifice	Pentobarbitalnatrium, 60mg/ml, Apoteksbolaget, Stockholm, Sweden
Fixative	250ml 0.4M phosphate buffer, Sigma-Aldrich Chemie GmbH, Steinheim, Germany 750ml distilled water 40g Paraformaldehyde, Sigma-Aldrich Chemie GmbH, Steinheim, Germany
Nissl Staining	Chloroform, 100%, Ethanol (99%, 95%, 70%, 50%) 1% Cresyl violet, Ethanol (50%, 70%, 95%, 99%), Acetic acid, 200ml Xylene All chemicals by Sigma-Aldrich Chemie GmbH, Steinheim, Germany
Cytochrome oxidase Staining	250ml 0.1% Cobalt chloride, 125ml Phosphate buffer 0.06mg Diamenobenzidine, 0,04mg Cytochrome c All chemicals by Sigma-Aldrich Chemie GmbH, Steinheim, Germany
Glucose	VWR International Ltd., Poole, England
Isoflurane	Isoflurane (Forene®), Abbott Scandinavia AB, Solna, Sweden
N_2O	AGA Linde Gas Therapeutics, Stockholm, Sweden
O_2	AGA Linde Gas Therapeutics, Stockholm, Sweden
Mineral oil Heating Blanket & Thermometer	DOW corning®f200/350cS fluid, BDH Lab. Supplies, Poole, England Harvard Blanket control unit, Harvard apparatus limited, Kent, England
Evaporator	Isotec 3, Cyprane, Keighley, England
Ventilator	KTR-4 Hugo Sachs Elektronik, Harvard Apparatus GmbH, March-Hugstetten, Germany
VSD Chamber	Optical Imaging, Rehovot, Israel

2.3 Hard- und Software

2.3.1 Setup

The animals were placed in a stereotaxic frame on a Nano-K floating Table (Newport Corporation, Irvine, California). Visual stimuli were presented on a 17" Sony Computer display (800*600pixels), refreshed at 120Hz, placed 57cm in front of the animal. Stimulation was controlled by VSG-package (Cambridge Research Systems, Kent, England) running on a Dell Pentium host computer. Source code was written by the author and a colleague using Pascal on a Borland Delphi 3 interface (Figure 6 shows the lab setup).

2.3.2 Voltage Sensitive Dye Imaging

A WuTech H469-IVR camera (WuTech Instruments, Gaithersburg, Maryland) with an array of 464 hexagonally arranged photodiode detectors (side length 2.1mm, diagonal length 4.2mm, detector size 162μm) and a RedShirtImaging®(RedShirtImaging, Decatur, Georgia) macroscope with 2x objective were used for optical imaging. Light from a 100W halogen lamp was filtered with a 630+/- 15nm band pass excitation filter and reflected onto the cortex (Figure 7). The epifluorescent image was

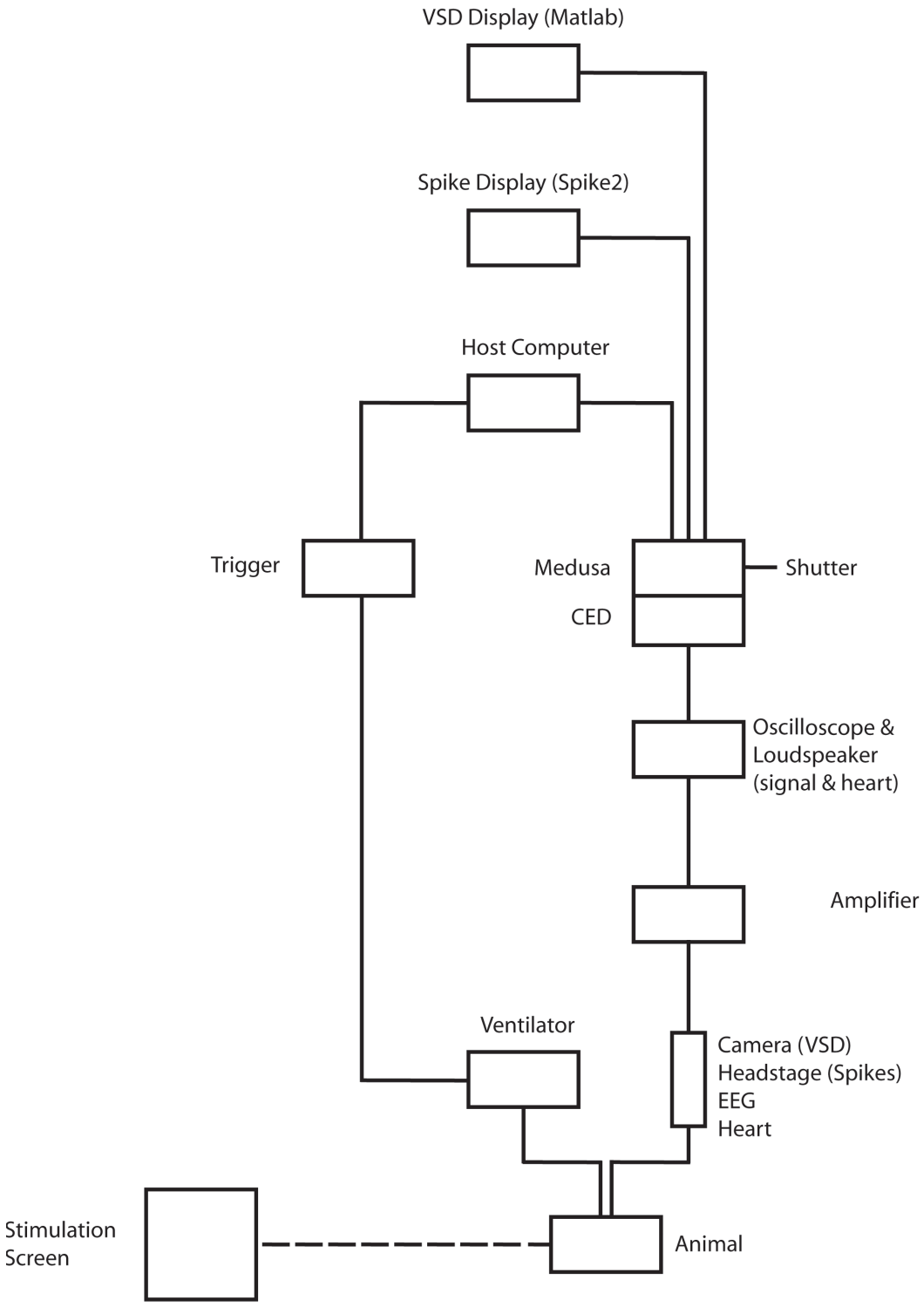

Figure 6: Plan of the lab setup for Voltage Sensitive Dye Imaging (VSD) and electrophysiological recordings (Spike).

passed through a 665nm long-pass acquisition filter and collected by the array detectors. Fluorescence signals from a hexagonal cortical area of diagonal length 4mm were collected with 0.61ms duration frames. VSD data was acquired with WuTech, RedShirtImaging®, software on a Dell Pentium 4 Computer. EEG, heart trigger, ECG and respiration were recorded and controlled by Spike 2 Software (Cambridge Research Systems, Kent, England) running on a Dell PC. Image acquisition was triggered to the heartbeat to improve signal to noise ratio. Internal pictures were taken with a Panasonic CCD camera (CCTV camera, WV-BP332, Matsushita, Laguna, Philippines). Pictures were processed with Adobe Illustrator CS2 on a Dell Latitude Pentium 4 notebook.

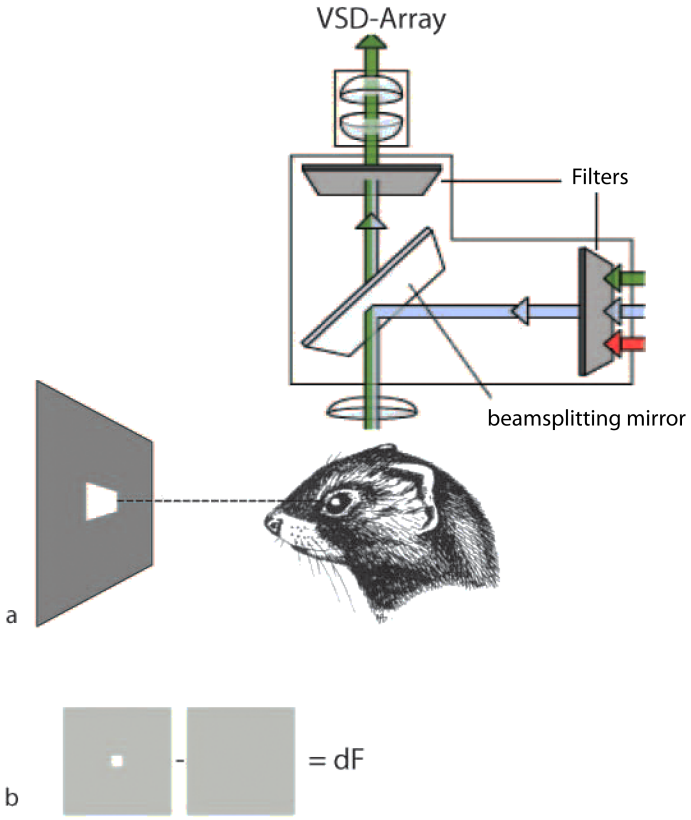

Figure 7: The experimental setup for Voltage Sensitive Dye Imaging. a. The animal is placed in front of the monitor where the visual stimuli are presented. Visual cortical responses lead to changes in fluorescence characteristics of the dye. While illuminating the cortex with a lamp (not shown) the reflected light is filtered and captured by the VSD array. b. The stimulus and blank conditions are shown. Cortical responses to the blank condition are subtracted from responses to the stimulus condition leading to dF, the change of fluorescence displaying the change of cortical activity evoked by the stimulus alone.

2.3.3 Electrophysiology

For the receptive field mapping multi unit activity was recorded with a monopolar tungsten electrode (FHCinc, Bowdoin, Maine) with a tip resistance between 0.8 and 1.2 MOhm. The signal was filtered between 100Hz and 10kHz and amplified with

a gain of 10kHz. Reference was attached to the animal's neck muscle. Receptive field position was determined using Matlab®Version6 (the MathWorks, Natrick, Massachusetts). During electrophysiological experiments (Figure 8) the action potentials of multiple neurons were recorded with two electrode arrays. Each array was made up of eight monopolar tungsten microelectrodes (FHCinc, Bowdoin, Maine) with a tip resistance between 0.8 and 1.2 MOhm. Electrode spacing on the arrays was ca. 400μm. Reference was attached to the animal's neck muscle. Signals were amplified and conditioned using a preamplifier and amplifier (16 channel Medusa, Medusa Base station, Tucker-Davis Technologies, Alachua, Florida) attached to a head stage (Tucker-Davis Technologies, Alachua, Florida). Signals were band-pass-filtered (100Hz-10kHz) online (Gain 200*200K) and subsequently acquired using an A/D-converter (CED power 1401, Cambridge Research Systems, Kent, England) controlled by Spike 2 Software (Cambridge Research Systems, Kent , England) running on a Dell PC. During recoding signals from one of the channels were played through a loudspeaker (AM 8 Audio Monitor, Grass Medical instruments, Quincy, Massachusetts).

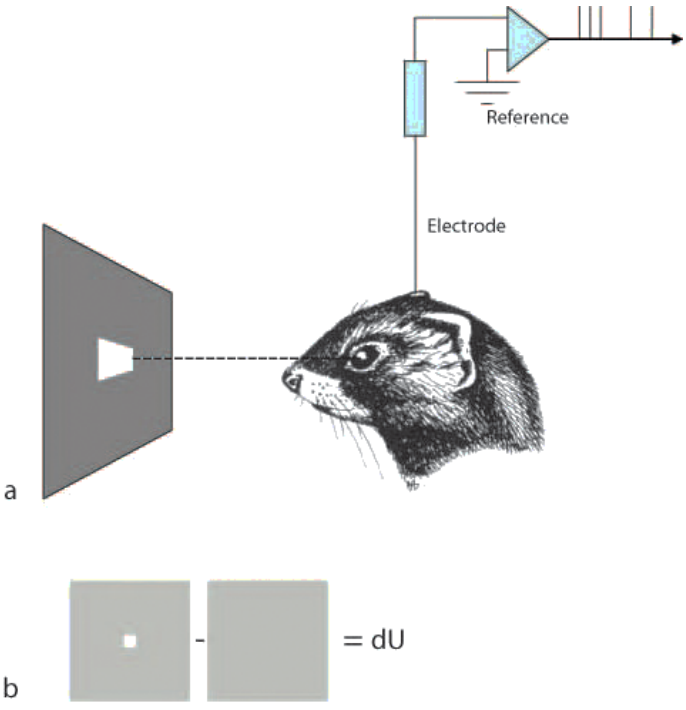

Figure 8: The experimental setup for recording multi unit activity. a. The animal is placed in front of the monitor on which the visual stimuli are presented. Multi unit activity is recorded from several sites of the visual cortex. The reference electrode is connected to a muscle. b. The stimulus and blank conditions are shown. Cortical responses to the blank condition are subtracted from responses to the stimulus condition leading to dU, displaying the change of cortical activity evoked by the stimulus alone.

2.4 Experimental Procedures

2.4.1 Preparation

At the beginning of the experiment the animal was initially anaesthetized with intramuscular doses of 0.34mg/kg Medetomidinhydrochloride, 12.5mg/kg Ketaminhydrochloride and 0.19mg/kg Atropine. An intravenous canula was secured into an arm vein. After tracheotomy a metal respiratory tube was inserted into the trachea for ventilation. Then the ferret was placed on a floating table. The respiratory tube was connected to a ventilator. The animal was artificially ventilated with 1% Isoflurane and a mixture of 1:1 nitrous oxide and oxygen. Expiratory CO_2 was measured and kept between 3.5-4.5%. ECG electrodes were connected to thoracic muscles. Body temperature was controlled with a rectal thermometer and maintained at $37°C$ with a heating blanket. Nutrition was held up with intravenous injections of 1ml of a 10% glucose solution five-hourly. The head was mounted into a stereotaxic frame fixed on the table. The skin of the skull was incised above the sagittal suture and the temporal muscles were deflected on both sides. The animal received an intravenous injection of a corticosteroid-solution (1.25mg/kg) to prevent brain swelling and oedema during craniotomy. On the right side of the scull a screw was put into the bone to record the EEG during VSD recording. On the left posterior part of the scull a circular craniotomy (1cm in diameter) was performed above the visual cortex. After the craniotomy a circular stainless steel optical pressure chamber was cemented to the cranium and sealed up with dental acrylic. The dura mater was removed to expose the cortex. The suprasylvian and lateral sulcus as well as the dorsal border of the brain were visible after the craniotomy in all cases. The cortex was covered with artificial cerebrospinal fluid to prevent it from drying out. A photo of the intact brain surface was taken with an external camera while illuminating it with a green light to emphasize the vascular pattern (Figure 9). The cortical representation of the area centralis was identified and marked on the external picture. According to Manger et al. (2002) this point was supposed to be situated on the vertical meridian. As a primary guide to determine the center of field of view an artery that came from the suprasylvian sulcus and ran towards the vertical meridian was used.

The ferret was moved under the macroscope and an internal picture of the cortex was taken with a CCD-camera, displaying the cortical representation site of the area centralis in the upper middle part of the hexagon. Since the internal CCD- and array-camera had the same optical axis the representation of the area centralis, as well as the vertical meridian and the higher order areas were imaged by the array. During the preparations the ferret's eyes were protected by frequent covering with drops of a 0.9% saline solution. The pupil of the right eye was dilated and accommodation was paralyzed with Atropine eye drops. The nictitating membrane was retracted with Phenylephrine eye drops. A zero power contact lens was placed on the cornea. The left eye was occluded. The animal was paralyzed with an ini-

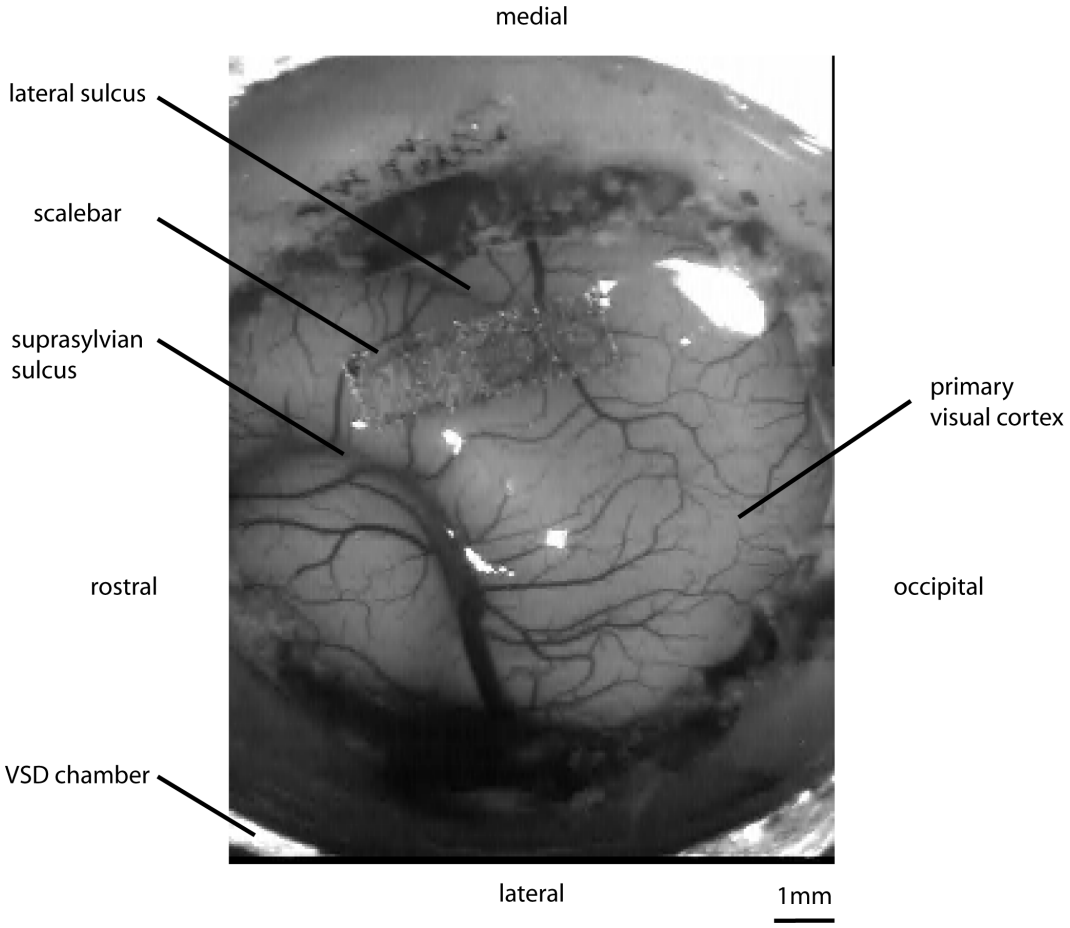

Figure 9: A photograph of the intact brain surface. The dura was removed and the brain covered with ACSF. The visual cortex was exposed, lateral and suprasylvian sulcus were marked. At the edges of the image parts of the chamber that was cemented to the skull are visible. A scale bar was put into the chamber on the ACSF surface.

tial intravenous bolus injection of Pancuroniumbromide. After that paralysis was maintained by continuous transfusion of Pancuroniumbromide in NaCl-Solution. Throughout the experiment the anaesthetic level was monitored by means of heart rate and EEG. Then the receptive field of the representation of the area centralis was mapped. Therefore, a single microelectrode was lowered into the cortex. A computer screen was placed 57 cm in front of the ferret's right eye. Stimulation was provided monocularly through the contralateral (right) eye. Vertical (20 pixels width) and horizontal (20 pixels height) bars and a single square of (40*40 pixels) of both 100% and 60% contrast were moved across the screen using a manual receptive field mapper. The responses to these stimuli were recorded to approximate the location of the cells' receptive field. The position of the screen was adjusted for the stimuli exciting the cells to be shown in the center. To confirm the correct placement of the screen a receptive field mapper program (Jones and Palmer, 1987) was run. It showed a chessboard pattern consisting of rapidly flickering (120Hz) random black and white dots. Neuronal activity was recorded with the single electrode and response patterns were correlated to the corresponding pictures. Like this the point on the screen that evoked the clearest responses was displayed as the representation

of the receptive field (Figure 10). After the point of the most distinct response was found the position of the screen was readjusted, if necessary, to make sure the receptive field was centered on the screen. The relative position between animal and screen was marked on the screen with a laser fixed on the stereotaxic frame close to the ferret.

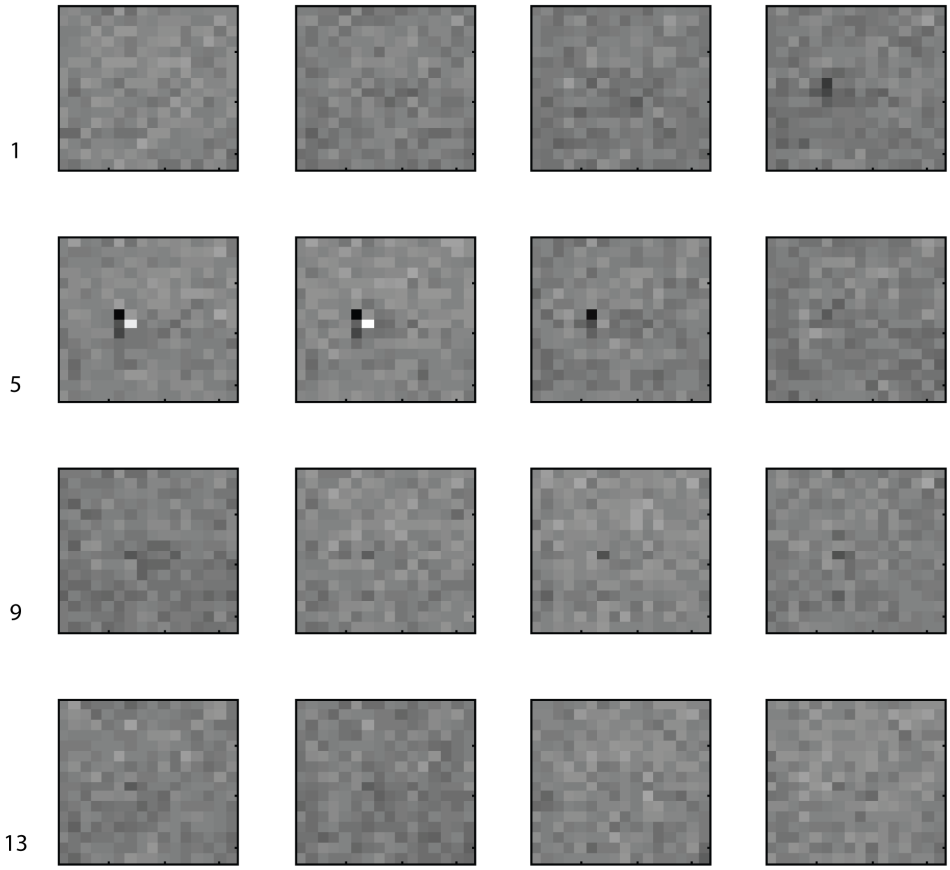

Figure 10: The result of one receptive field mapping. The screen is divided up in 16*16 squares, randomly changing luminance from black to white and back. The number of spike trains is recorded at the estimated cortical representation of the center of visual field. The arrangement of black and white squares is correlated to the number of spike trains recorded during the mapping. The highest response rate is displayed as white, the lowest response rate is displayed as black. Values in between are distributed along a greyscale. In this animal the highest response rate was achieved when presenting white squares close to the center of the screen, shifted towards the left edge by approximately 1 square (white spot), The lowest response rate was achieved in the direct surrounding (black spots) agreeable to a lateral inhibition. On the rest of the screen displaying black or white squares resulted in a small random amount of spike trains. Each of the 16 pictures shows the response pattern at an additional time lag of 10ms after stimulus onset. The center of visual field is first visible in the 5th picture, i.e. time lag for stimulus response is approximately 50ms and lasts for about 30ms, This is within the expected range of latency to response onset and response duration.

The chamber was filled with VSD and the exposed cortex was stained for two hours. During this time the hexagonal area of the cortex that was going to be imaged with the array camera was estimated using the internal picture taken by the CCD camera. Since both cameras share their optical axis it was possible to project the edges of the hexagon of photodiodes of the array camera onto the cortex picture. This information was used to place the electrodes during electrophysiological recordings. After the staining the dye was removed and the brain rinsed with ACSF. The chamber was filled with mineral oil. A cover glass was screwed onto the chamber under light compression. This caused pressure to build up inside the chamber decreasing pulsation artefacts due to heartbeat and respiration. The ferret was moved under the macroscope and the cortex was adjusted and focused with the CCD camera. Changes in the previously determined position of the animal were precluded by comparing the image to the first internal picture. The screen was moved to the appropriate place aligning it to the laser mark that had been taken before. After focusing the camera on the cortical surface the ferret was moved up by 300 micrometers to collect fluorescence signals from deeper cortical layers and to reduce artefacts caused by the cortical vessels.

2.4.2 Visual stimulation

A full screen random dot background, dot size one pixel, luminance 14.6cd was shown to the animal. This background remained during all trials. Four different stimulus conditions were shown. Condition one was a control condition, presenting only the background. Conditions two to four were stimulus conditions with white squares, 100 by 100 pixels in extension (according 3.7° by 3.7°, viewed from a distance of 57cm), appearing in the center of the screen. The square moved upwards, downwards or remained stationary. Luminance of these squares was 41.4cd. Thus luminance contrast between stimulus and background was 48%. Stimulus velocity was 24.5 degrees per second. The moving squares travelled 12.9 cm across the screen. For all three conditions the stimulus was shown for 550ms. Each stimulus was presented once per trial.

2.4.3 Voltage Sensitive Dye Imaging

During the imaging a unipolar EEG was monitored with reference to a muscle. While presenting visual stimuli on the monitor the dye was excited and responded with changes of fluorescence characteristics. The array camera detected these changes. Data acquisition was triggered on the animal's heartbeat. Respiration was stopped and anaesthesia-level decreased during stimulation. The five stimulus conditions were shown randomly, each condition was shown five times per recording session. During stimulus presentation the cortex was lit up with a lamp (Figure 11). An electromechanical shutter limited the duration of illumination. Data acquisition started 200ms before stimulus onset and stopped 250ms after stimulus offset.

Stimulus duration was 550ms. The array camera took a sequence of images (16 kHz) of the cortex during the acquisition time. The images were digitized and stored on a computer. Five trial repetitions were shown per session, ten VSD-sessions were recorded, resulting in a total of 50 repetitions of each condition. Before the first and after the last trial an NRLI (Normalized resting light intensity) trial was run to rule out unevenness of the brain surface and staining when analyzing the data. After the imaging the brain was rinsed and covered with ACSF.

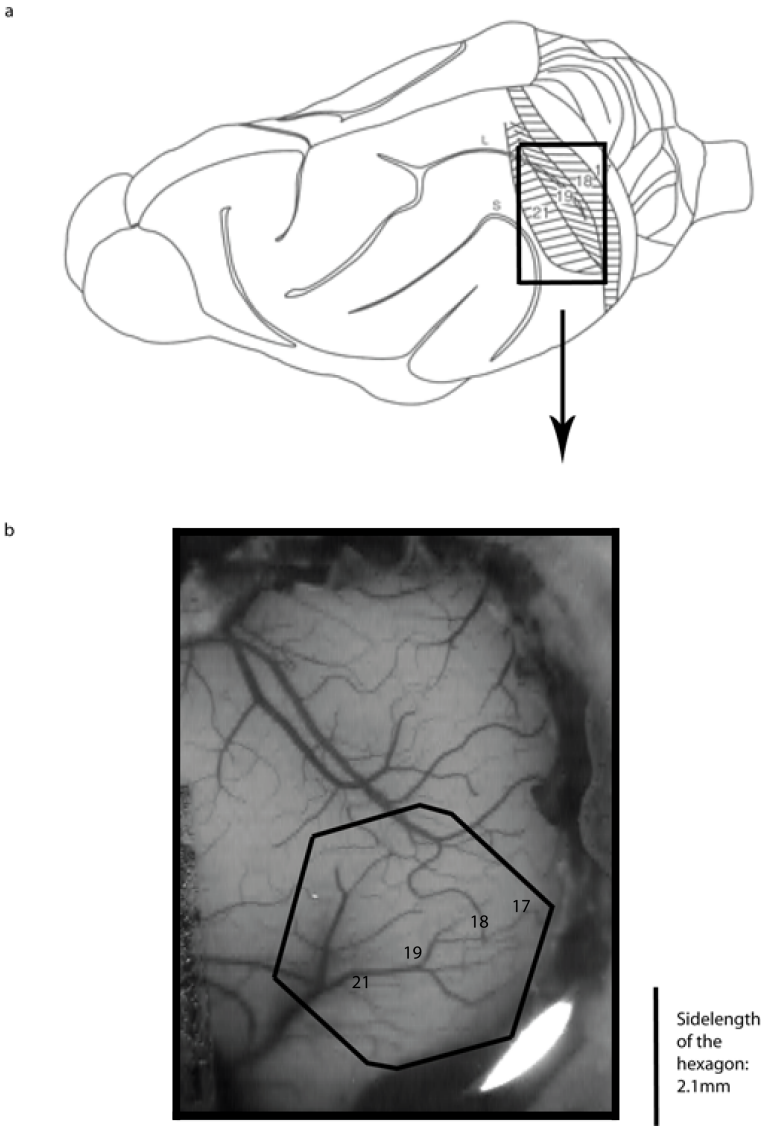

Figure 11: The cortical area imaged by the array camera. a. A figure of the ferret brain (left hemisphere) as shown in the introduction. Areas 17, 18, 19 and 21 are marked. L: lateral sulcus, S: suprasylvian sulcus. The marked part is enlarged in b. b. The area marked in a in a photo of the ferret brain. The lateral and suprasylvian sulcus as well as visual areas 17, 18, 19 and 21 are exposed. The hexagon marks the area that is imaged by the array camera.

2.4.4 Electrophysiology

16 electrodes were lowered into the cortex with two micromanipulators (Figure 12). The recorded signal was amplified, filtered and visualized on a computer screen as well as played through a loudspeaker. One array with 8 electrodes was placed along the vertical meridian at the 17/18-border, perpendicular to the cortical surface. The other electrode array with 8 electrodes was placed orthogonally to the first one in the higher order areas. The position of the second array was changed in between sessions in order to cover as much space as possible. The first array was not moved. For each electrode position 160 (4 conditions*40 repetitions) trials were displayed randomly and neuronal activity was recorded. After each session the screen positions "seen" by the responding neurons were detected with the receptive field mapper program. Using the map of the hexagon on the cortex picture that had been prepared during staining the electrodes could be positioned inside the hexagon to spatially correlate the VSD- and electrophysiology-data.

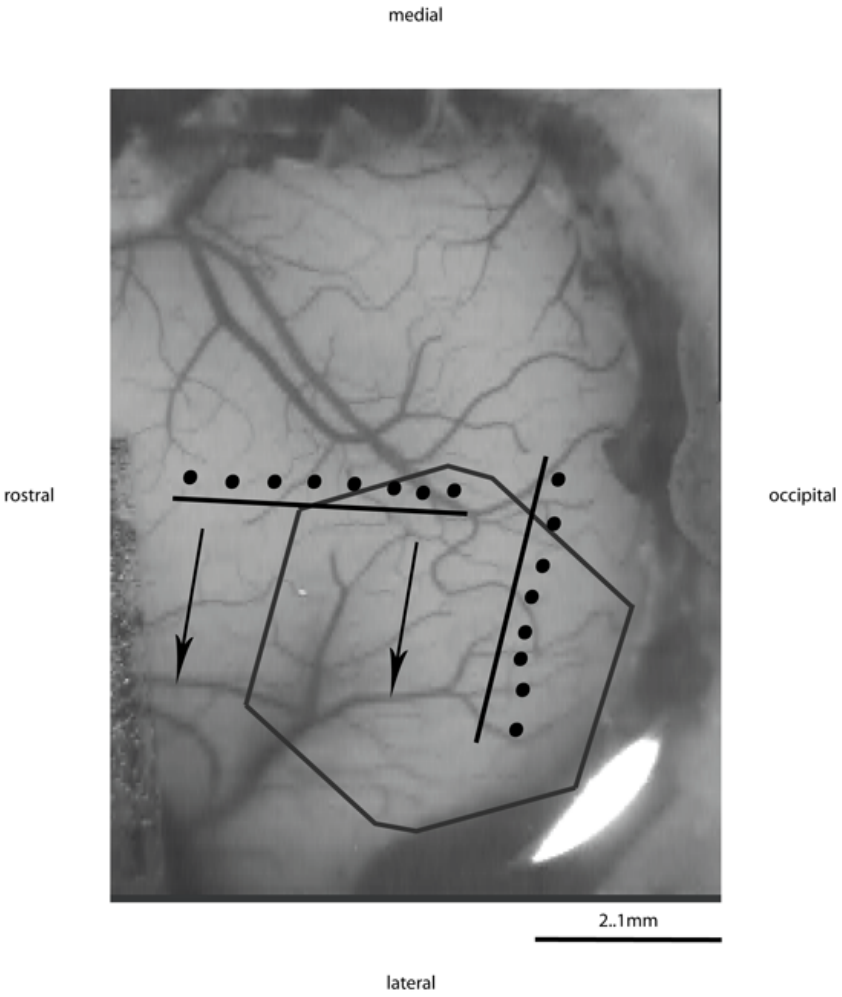

Figure 12: The penetration pattern of the electrodes. As in figure 11 the hexagon shows the area that was imaged by the array during VSD recordings. Array 1 (8 electrodes) is placed at the assumed location of the 17/18 border. Array 2 (8 electrodes) is placed perpendicular and rostral to Array 1, in areas 18, 19 and 21. To cover the whole area that was imaged with VSD Array 2 was moved after each recording session as indicated by arrows. Six to ten recording sessions were performed, each with a different position of Array 2.

After recording the electrode positions were marked on the external picture and current was passed trough the electrodes (1μA for 1s), to leave coagulation marks. Three vertical needle marks were placed around the recording site. These marks were later used to reconstruct electrode positions and correlate the alignment of the histology pictures to the pictures of the cortex. The animals were sacrificed with an overdose of intravenous pentobarbital and perfused intracardially with 1l of 0.9% saline and 1l of 4% Paraformaldehyde in 0.1M phosphate buffer. The brain was taken out and fixed in Paraformaldehyde overnight (at 5°C) and in a 30% glucose solution until sectioning (at 5°C).

2.5 Data Analysis

2.5.1 Voltage Sensitive Dye Imaging

All data was processed with Matlab®, version6 (The MathWorks, Natrick, Massachusetts). For each channel the VSD-signal for the control condition was subtracted from the signal for the stimulus condition to eliminate respiration and heartbeat artefacts: V(t)Ch,Stim-V(t)Ch,Ctrl = ΔV(t)Ch. An average of both NRLI recordings was calculated. Each frame of the signal was divided by the corresponding averaged NRLI frame (F0Ch). ΔV(t)Ch/ F0Ch =ΔV(t). All signals were time filtered (Gaussian filter, σ=12.3ms) and inverted so increase in luminance represented an increase in activity. The responses to the different conditions were averaged across all repetitions and sessions. All data files were cut after 950ms to remove artefacts caused by the shutter closing at 1000ms. This signal was called the absolute signal and is referred to from now on unless stated otherwise. Signal onset at one representative channel for both area 17/18 and 19/21 was detected. The averaged ΔV(t) signal was assumed to follow a Gaussian distribution. The fluctuations in the prestimulus period were used to estimate the p-value. At both sites significant response onset and 90% peak latency were detected with a p-threshold of 0.001 for the stimulus conditions. Using the latency to onset timings and distance between both sites the velocity of feed forward depolarization was calculated. VSD-responses at the channels along the 17/18 border (including the channels corresponding to electrophysiology representation sites) were analysed. Using a p-threshold of 0.001 significant response onset and 90% peak latency were detected across these channels for the motion conditions. Spatial local maxima were detected in the VSD files (neighbourhood-size: five channels) and data was spatially filtered over six channels. Then the dynamics of the VSD response to the moving stimuli were investigated by detecting the center of gravity in areas 17 and 18. The signal was time filtered (Gaussian filter, σ=3.1ms); the seven strongest activations were considered to determine the center of gravity. Using the distance between first and last channel as well as the difference in onset timing between them the velocity of the signal moving across these channels was calculated. Response behaviour at the second stimulus representation site at the 19/21 border was investigated for the motion conditions.

Therefore, a mask was overlaid the area of interest and response dynamics was examined under this mask.

2.5.2 Electrophysiology

All data was processed in Matlab®, version6 (the MathWorks, Natrick, Massachusetts). A Poisson distribution was fitted to the spike trains in the prestimulus period and spikes from the background trial. Spike trains showing a significantly increased discharge rate compared to both the prestimulus period and the background condition of $p<0.01$ were considered statistically significant periods of firing. Data was time filtered with a bin width of 20ms. Receptive fields of units for all electrodes were determined using the receptive field mapper program as described before. Therefore, it was possible to reconstruct the representation area of a given unit on the stimulation screen. The electrode placed at the representation of the area centralis was determined by the receptive field mapper program, the response latency timing of electrophysiology and VSDI and anatomical landmarks. With a p-threshold of 0.01 significant onsets and 90% peak latency were detected for all electrodes for both motion conditions and the stationary condition in all animals.

2.5.3 Histology

Three horizontal needle marks were made to align pictures of the slices after sectioning. The brain was cut frozen with a microtome (Leica SM200R, Leica Microsystems, Solms, Germany) at 50μm in a parasagittal plane. Sections were mounted on glass slides. Alternate sections were stained for cell-bodies (Nissl, Cresyl violet) and cytochrome oxidase. Images of the slices were acquired with a digital camera (Leica Camera AG; Solms, Germany). Visual areas 17, 18, 19 and 21 were distinguished by means of cytoarchitecture and cytochrome oxidase reactivity. Area borders were marked on the pictures with Adobe Photoshop (Figure 13). Horizontal needle marks were used to realign the sections with matlab. Using sulcal patterns, electrode and needle marks as well as vascular patterns the aligned borders were matched to the photograph of the brain surface. Patterns of the areal borders were laid over the VSD-movies.

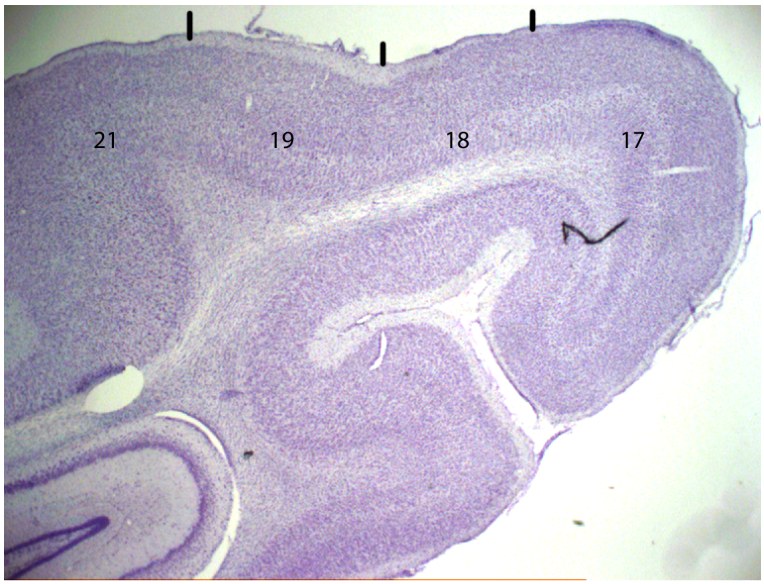

a

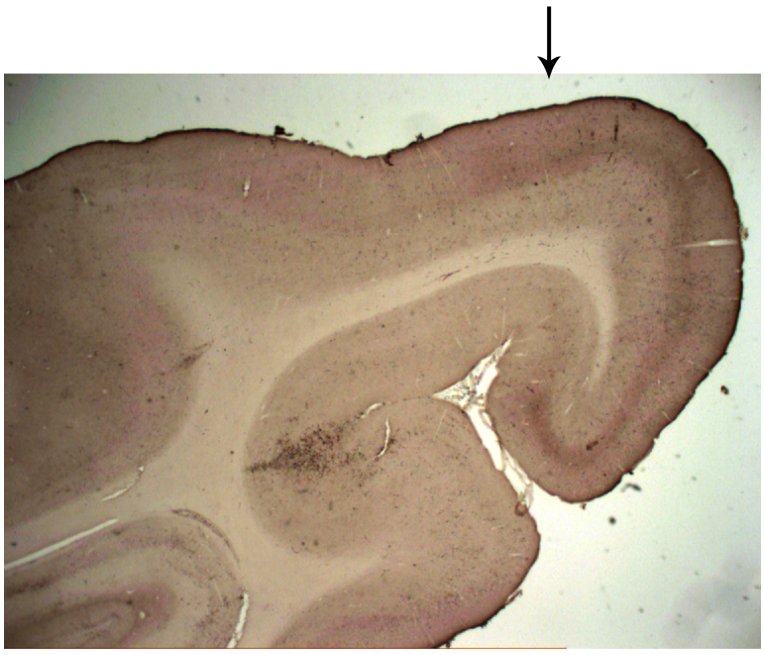

b

Figure 13: Two adjacent sections of the ferret visual cortex stained for Nissl substance (a) and cytochrome oxidase (b). Black marks in (a) show the areal borders, areas are marked in the section. Arrow in (b) shows the end of a strongly labelled band of cytochrome oxidase marking the border between areas 17 and 18.

3 Results

3.1 Voltage Sensitive Dye Imaging

3.1.1 Response detection at the initial stimulus representation site at the 17/18 border

When presenting a single moving or stationary white square in the center of visual field of the ferret the square was mapped to the border between cortical areas 17 and 18. This resulted in increased membrane potential of populations of neurons at the initial retinotopic site for both moving and stationary stimuli. The changes in membrane potential caused a decrease in fluorescence signal $\Delta V(t)$ when imaging with the Voltage Sensitive Dye RH 1838. After inverting the signal it showed an increase with population membrane potential in the representation locus (Table 4, 5).

Table 4: Significant response onset latencies (ms) for the initial activation in the center of visual field (mean values calculated for each animal) at the 17/18 border

Animal	*Onset (Upwards)*	*Onset (Downwards)*	*Onset (Stationary)*
1	no significant onset	no significant onset	no significant onset
2	48	51	40
3	31	20	109
4	34	37	33
5	23	35	36
6	25	46	77
Average	32.2	37.8	59.0
Standard deviation	9.9	12.0	33.3

The significance of the difference between response onset latencies for the motion conditions as opposed to the stationary condition was checked with a two-tailed t-test. There was no statistically significant difference for response onset latency between the upwards moving square and the stationary square ($p=0.24$). Neither was there a statistically significant difference for response onset latency between the downwards moving square and the stationary square ($p=0.34$).

Table 5: 90% peak latencies (ms) for the initial representation site (mean values calculated for each animal) at the 17/18 border at the same array channel as in table 3.1

Animal	*Latency (Upwards)*	*Latency (Downwards)*	*Latency (Stationary)*
1	102	No significant peak	No significant peak
2	272	101	427
3	217	126	117
4	59	58	No significant peak
5	85	99	70
6	98	98	No significant peak
Average	138.8	96.6	204.3
Standard deviation	85.3	24.7	194.4

Differences in latency to 90% peak (Table 5) for the moving as opposed to the stationary conditions were not determined here since the condition displaying the stationary square only showed significant peaks in three animals.

3.1.2 Response detection along the vertical meridian in areas 17/18 for the moving stimuli

When presenting a stationary square the signal is mapped to the representation site on the vertical meridian in areas 17/18 after some 30-40ms (Figure 14, 15). The center of representation of the signal did not move although $\Delta V(t)$ showed an increase along the vertical meridian in both directions. When presenting a moving stimulus the initial mapping at the stimulus representation site occurred at the same position with the same temporal delay. However, the center of gravity of activity showed the following behaviour: For the upwards moving square, in five out of six animals the center of gravity showed a movement towards lateral positions along the 17/18 border (Figure 16). In one animal the center of gravity showed no motion. For the downwards moving square, in four out of six animals the center of gravity showed a movement towards positions medial to the initial representation site (Figure 17). In two animals the center of gravity showed no motion.

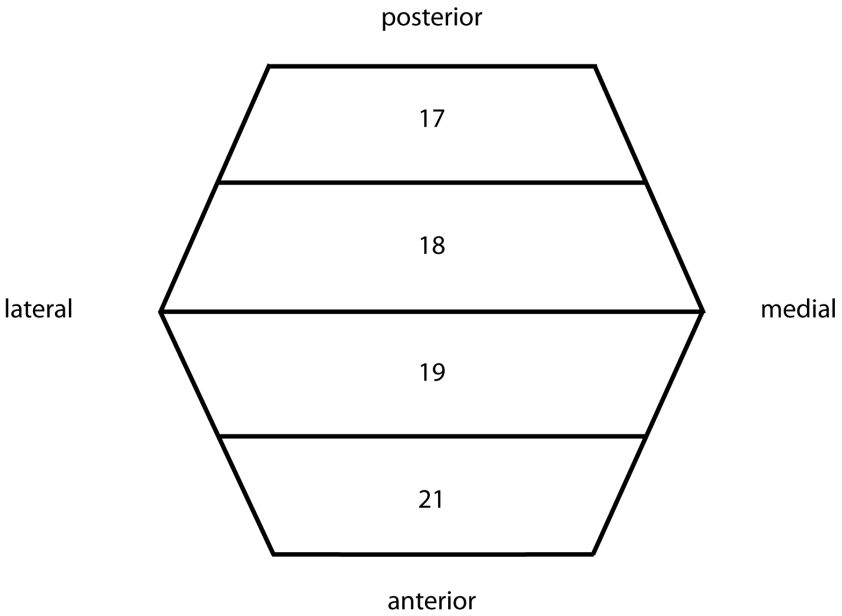

Figure 14: The arrangement of the hexagon shown in Figures 15 to 17

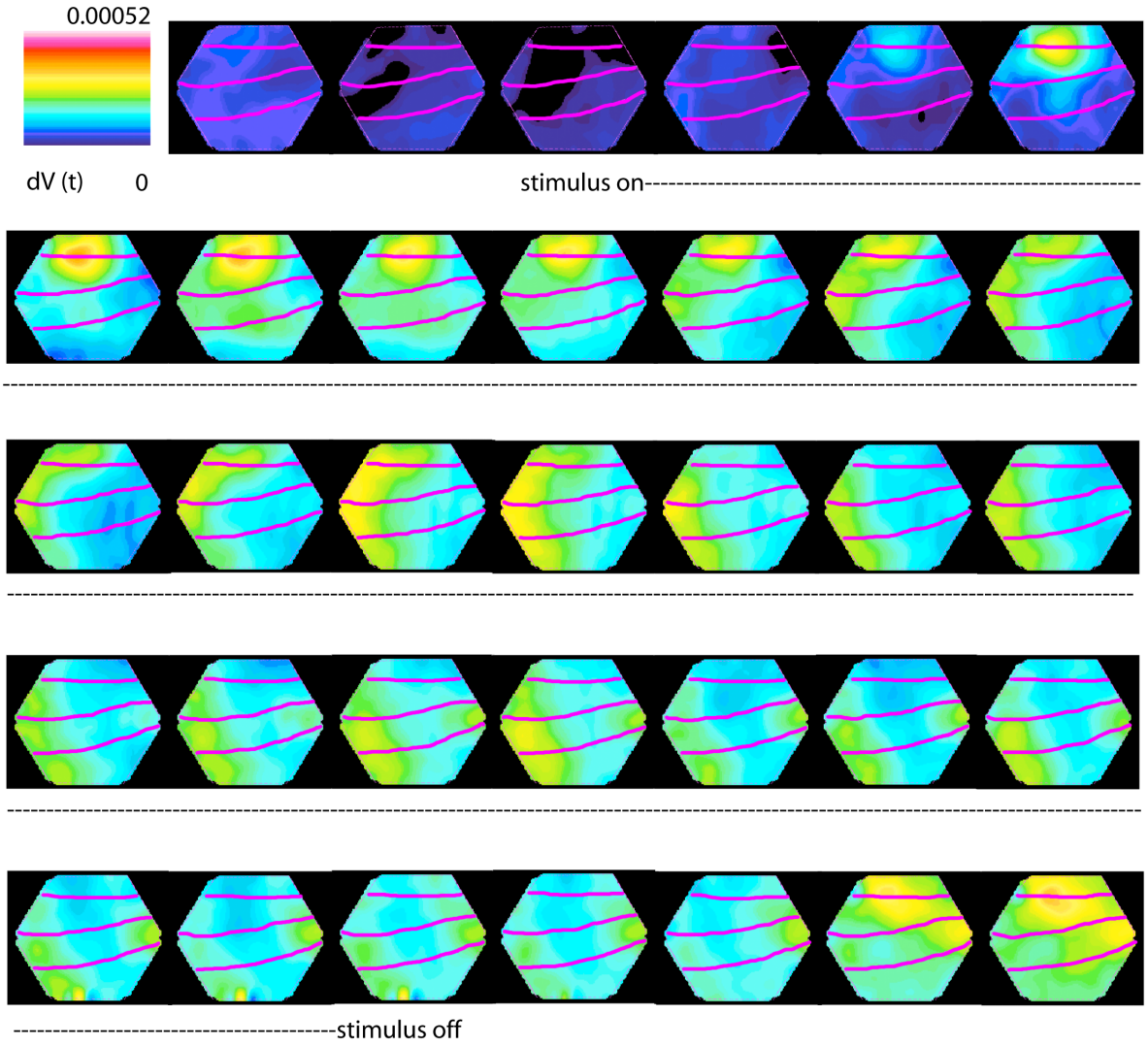

Figure 15: The response of the visual cortex to the stationary square acquired with VSD imaging. The hexagon of the array camera was placed above the visual cortex. Purple lines indicate the borders between areas 17, 18, 19 and 21. Area 17 is on top, area 21 on the bottom of the hexagon. The lateral part of the imaged area is displayed on the left, the medial part on the right half of the hexagon. Each little picture shows a screenshot of the movie taken by the array camera with a 20ms time delay between each picture. Stimulus on- and offset times are marked. Activity (dV (t)) is color-coded as shown by the scales. Note the onset of response approximately 40ms after stimulus onset at the 17/18 border, approximately 60ms after stimulus onset at the 19/21 border. For the stationary square there is an off-response at the same positions with temporal delay similar to that of the on-response.

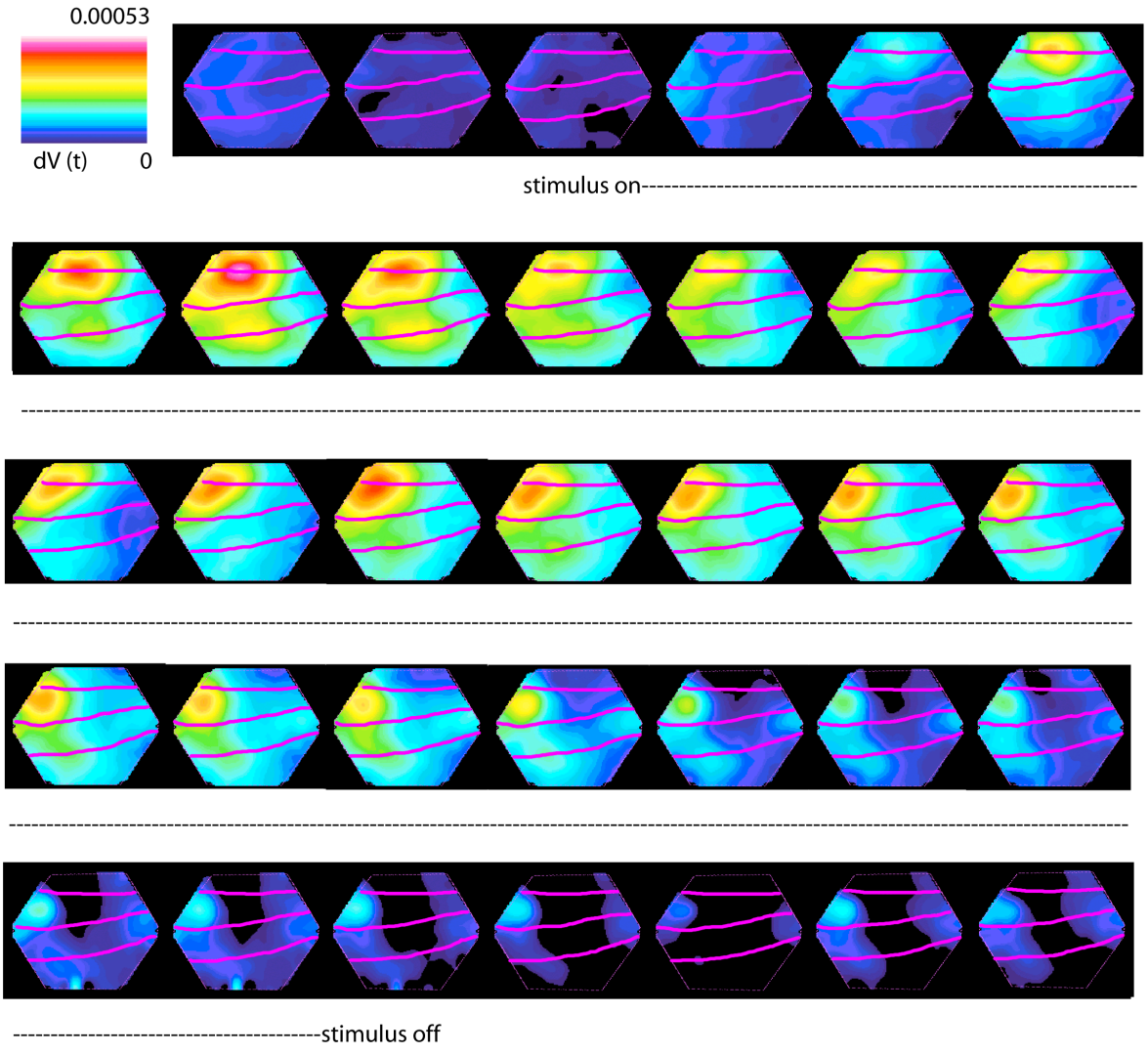

Figure 16: The response of the visual cortex to the upwards moving square acquired with VSD imaging.. Caption as in figure 15. The response onset occurs approximately 40ms after stimulus onset at the 17/18 border, approximately 60ms after stimulus onset at the 19/21 border. For the upwards moving square activity travels to the left half of the hexagon which images subsequent lateral positions on cortex.

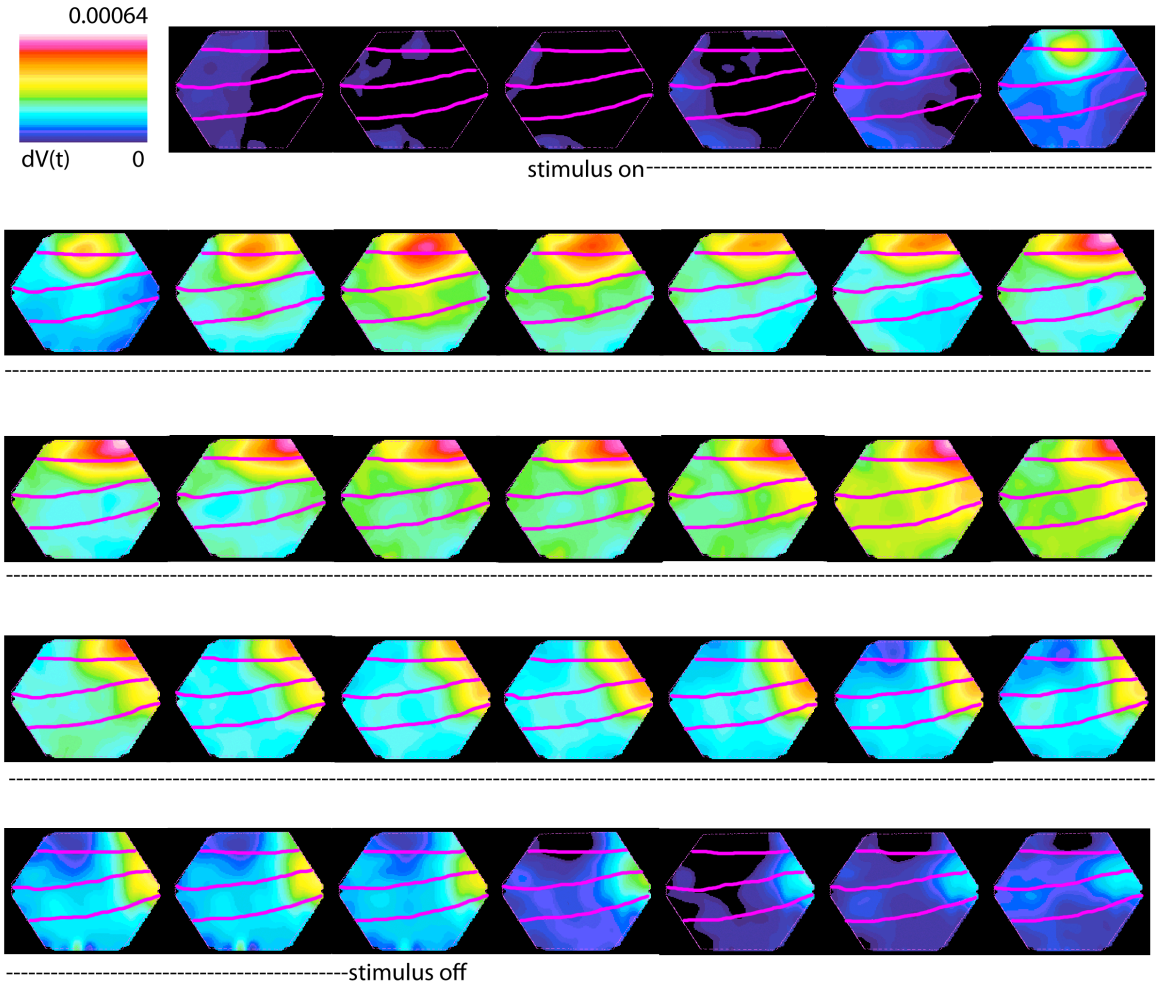

Figure 17: The response of the visual cortex to the downwards moving square acquired with VSD imaging. Caption as in figure 15. The response onset occurs approximately 40ms after stimulus onset at the 17/18 border, approximately 60ms after stimulus onset at the 19/21 border. For the downwards moving square activity travels to the right half of the hexagon which images subsequent medial positions on cortex.

The velocity of motion along the 17/18 border was calculated. Spatial local maxima were detected for both motion conditions in each animal. Response onset time at the initial representation site was determined. Then, response onset time at a second channel, representing a more peripheral representation of the vertical meridian along the motion trajectory, was determined (Figure 18, 19). The time difference between activity peaks at the two channels that showed the local maximum of the stimulus representation site was calculated. The result was divided by the distance between both channels.

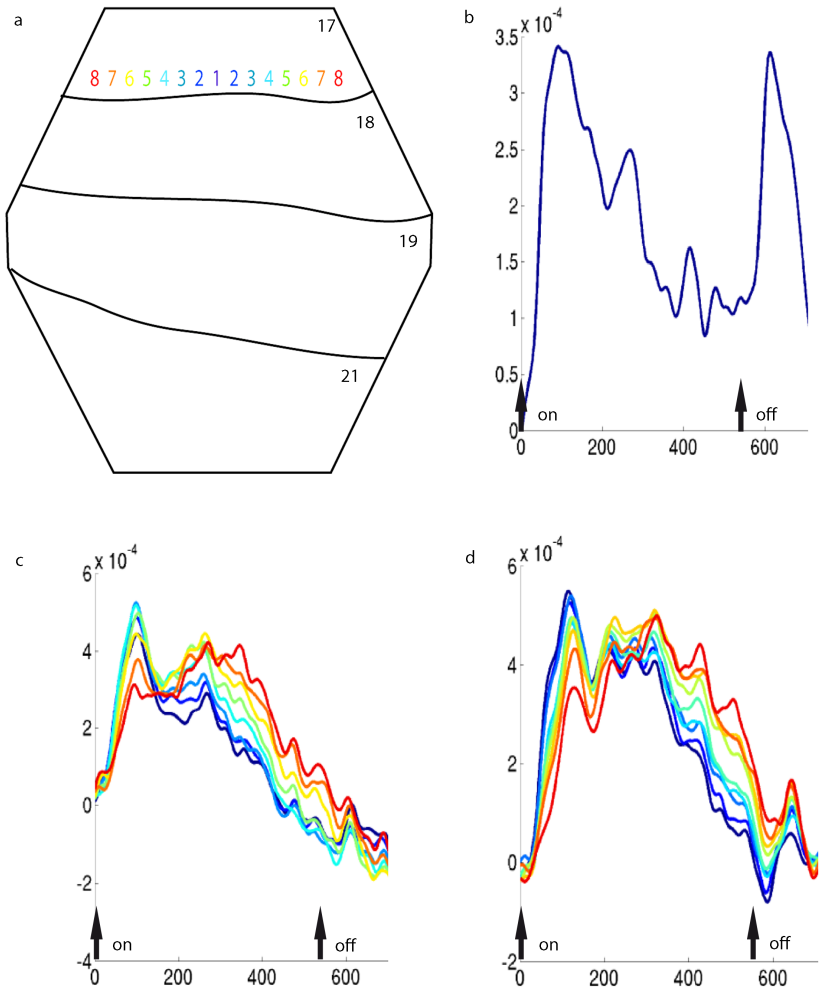

Figure 18: Response signals detected at several channels on the 17/18 border. a. Hexagon with areas 17, 18, 19 and 21 as shown before. Black lines indicate area borders. Number 1 (dark blue) shows the initial representation site of stimulus onset. Numbers 2 to 8 (light blue to red) show subsequent representation sites for the moving stimuli. Numbers on the right show cortical positions more medial, numbers on the left positions more lateral to the initial representation site. b. Response pattern of a single array channel at the initial representation site for the stationary condition; x-axis shows time in ms, y-axis shows change of activity dV (t). Stimulus onset at 0ms, offset at 550ms (indicated by arrows). c. Response pattern evoked by the upwards moving square; designation as in b). Responses are shown for channel 1 (dark blue) and 7 channels at subsequent lateral positions (light blue to red). d. Response pattern evoked by the downwards moving square; designation as in b). Responses are shown for channel 1 (dark blue) and 7 channels at subsequent medial positions (light blue to red).

The stimulus velocity calculation between channels resulted in a mean velocity of 5.4μm/ms (standard deviation 1.5μm/ms) for the upwards moving square (six animals) and in 7.5μm/ms (standard deviation 1.2μm/s) for the downwards moving square (six animals) on the 17/18 border. Assuming that five degrees of visual angle are mapped on one mm of cortex this results in a mean velocity across cortex of 27°/s (standard deviation 7.9°/s) for the upwards moving and 38°/s (standard deviation 6.2°/s) for the downwards moving square on the 17/18 border.

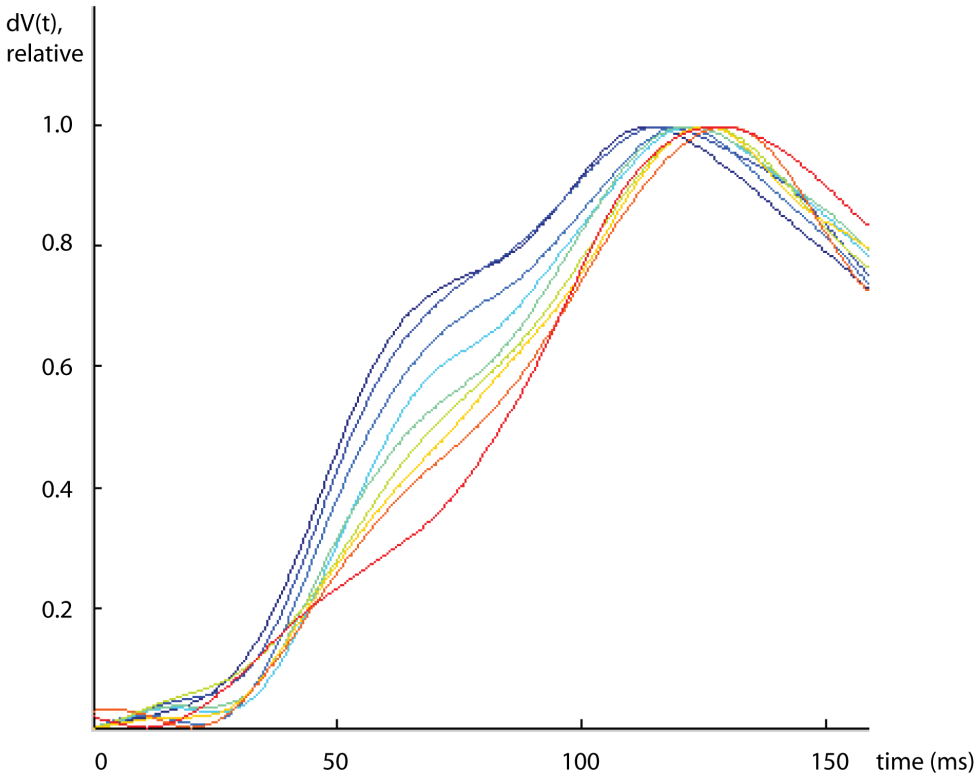

Figure 19: A magnified view of the response timing at the eight subsequent channels shown in Figure 3.4 a and d. Colour coding as in figure 18. Stimulus onset at 0ms. Signal strength is normalized to one in order to more clearly show the response onsets and peaks detected by the subsequent channels.

After determining the direction the activation takes across the imaged area with help of the center of gravity, the responses for the channels imaging the 17/18 border along the motion trajectory were investigated. For the upwards moving square response onsets showed subsequent increases of latencies for successive lateral positions in four out of six animals. In two animals the latency of response onsets increased from the lateral edge of the imaged area to the center position. 90% peak latency showed a subsequent increase of significant response onset time towards channels with positions lateral to the initial representation site in all six animals. For the downwards moving square response onsets showed subsequent increases of latencies towards medial positions in all six animals. 90% peak latency showed a subsequent increase towards lateral positions in all six animals.
As a next step the population membrane potential at the array channels spatially corresponding to electrode positions along the motion trajectory was investigated.

Since this analysis was done to compare the response behaviour between the two different recording methods, animal five was not included. VSD-Data was acquired for this animal, but no electrophysiology to correlate the recording sites to. The significant responses showed the following onset-latencies across array channels correlated to penetration sites: The upwards moving square evoked responses with onset latencies increasing with distance lateral from the center in two out of five animals. Latencies decreased towards more lateral positions in the three remaining animals. The downwards moving square evoked responses with latencies increasing with distance medial from the center in three out of five animals. Onset latencies decreased towards medial positions in one animal. One animal only showed significant onsets for one position, therefore no slope could be detected. The time to 90% peak showed the following latencies across array channels corresponding to penetration sites: For the upwards moving square the latency to 90% peak increased with lateral distance from the center in all five animals. For the downwards moving square the latency to 90% peak increased with medial distance from the center in four animals and decreased in one.

3.1.3 Response detection in higher order visual areas

3.1.3.1 Response detection at the initial representation site at the 19/21 border

When showing a stimulus in the center of field of view and imaging the cortex with Voltage Sensitive Dye it becomes obvious that the stimulus is not only mapped to a single cortical site. Rather it is mapped to two sites, at the 17/18 border and at the 19/21 border (Table 6, 7). The 19/21 border was imaged with Voltage Sensitive Dye in five out of six animals (1-3, 5, 6). For animal 4 the border was mapped to a position right outside the edge of the hexagon. Therefore a marginal channel of the hexagon was investigated instead, not exactly representing the border but being the closest possible point to inspect. Mean significance response onset times and latencies to 90% peak response were calculated both including and excluding animal 4.

Table 6: Significant response onset latencies of population membrane potential for the second activation site at the 19/21 border (mean values calculated for each animal)

Animal	*Onset (Upwards)*	*Onset (Downwards)*	*Onset (Stationary)*
1	88	18	113
2	48	49	39
3	85	102	No significant onset
4	61	88	58
5	43	55	63
6	64	75	No significant onset
Average	65.0	64.3	68.3
Standard deviation	18.5	30.2	31.5
Average excluding # 4	65.6	59.8	62.7
Stdev excluding # 4	20.6	31.2	43.6

Table 7: Time to 90% peak latencies of population membrane potential (mean values calculated for each animal) for the second activation site at the 19/21 border, same channel as in table 6

Animal	*Latency (Upwards)*	*Latency (Downwards)*	*Latency (Stationary)*
1	113	26	111
2	71	71	64
3	191	126.4	118
4	92	89	No significant onset
5	85	106	89
6	108	107	No significant onset
Average	109.9	87.4	95.6
Standard deviation	42.8	35.5	24.4
Average excluding #4	113.6	87.2	95.5
Stdev excluding #4	46.5	39.6	24.4

3.1.3.2 Connection of activity between the initial representation sites at the 17/18 and 19/21 borders A band of increased activity connecting the stimulus representation site at the 17/18 border to the one at the 19/21 border can be seen in the pictures of the array camera (Figure 20). It was now investigated whether this band of activity represents a subsequent increase of population membrane potential between the two representations of the center of field of view, originated in areas 17 and 18 and targeting the vertical meridian at the 19/21 border. Therefore the significant response onsets at channels imaging the areas between the two representation sites were detected for all animals and conditions (Table 8):

Table 8: Significant initial response onsets (ms) at three channels (1-3) between the 17/18 and 19/21 border. X: No significant onsets detected.

Animal	*Onset (Upwards)*	*Onset (Downwards)*	*Onset (Stationary)*
1	45, 90, X	30, X, X	204, X, X
2	47, 44, 42	49, 50, 67	37, 36, 34
3	02, 17, 22	12, 48, 15	48, 37, 97
4	39, 51, 54	42, 48, 50	37, 53, 57
5	28, 35, 41	39, 42, 52	35, 50, 57
6	37, 44, 46	53, 60, 42	X, X, 96

The direction the band of activity takes between the 17/18 border and the 19/21 border was investigated for all animals. This was done by assessing the response onset times of the channel representing the initial representation site at the 17/18 border, the channels between the 17/18 and 19/21 border and finally the channel representing the initial representation site at the 19/21 border. A slope of these response onset timings was calculated, positive slope meaning population membrane potential increased first at 17/18 and later at 19/21, negative slope representing the opposite. In 72.2% activity travelled from areas 17/18 towards areas 19/21 (Table 9).

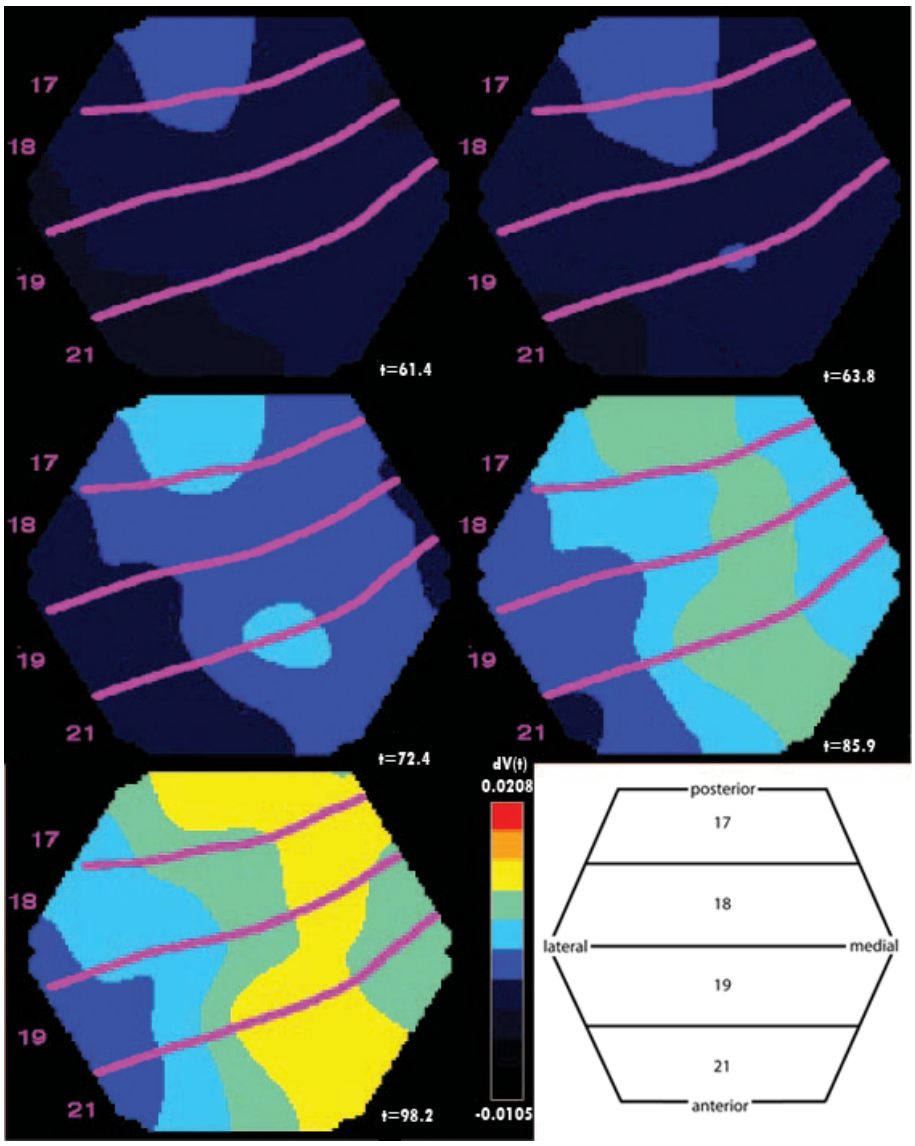

Figure 20: The band of activity connecting the two representation sites at the 17/18 and 19/21 borders. Each frame shows the response pattern at a given time (t in ms) after stimulus onset. Areas and borders are superimposed in magenta lines. Activity is colour coded as indicated by the scale bar. The figurine in the bottom right corner shows the orientation of the hexagon.

The significance of difference in onset timing at both representation sites was investigated: The significance of the difference between response onset latencies at the representation in areas 17/18 as opposed to the representation in areas 19/21 was tested with a two-tailed t-test. The response onset latency in area 19/21 was significantly higher than the one in areas 17/18 for the upwards moving square ($p=0.04$). For the downwards moving and the stationary square, the response onset tended to be later in areas 19/21, though the p-value was >0.05 ($p=0.07$, $p=0.19$, respectively). The difference between latencies to 90% peak at the representation site in areas 17/18 as opposed to the representation site in areas 19/21 was calculated with a two-tailed t-test. The time to 90% peak in area 19/21 was not significantly later than the one in areas 17/18 for the upwards moving ($p=0.45$), for the downwards moving ($p=0.77$), and the stationary square ($p=0.46$).

Table 9: Direction of population membrane potential connecting the initial stimulus representation sites (either 17 to 21 or 21 to 17)

Animal	*Direction (Upwards)*	*Direction (Downwards)*	*Direction (Stationary)*
1	17→21	21→17	21→17
2	21→17	17→21	21→17
3	17→21	17→21	21→17
4	17→21	17→21	17→21
5	17→21	17→21	17→21
6	17→21	17→21	17→21

3.1.3.3 Response detection along the vertical meridian in areas 19/12 for the moving stimuli The center of gravity of population membrane potential for areas 19/21 was detected. In some cases the response representation site was not stronger than the surrounding noise. In other cases there was a stronger activation but its center of gravity showed no motion. Therefore it was not possible to detect a motion pattern. In order to more carefully investigate if there was any motion of the signal along the vertical meridian in areas 19/21, the signal acquired by the channels above the border was investigated separately from the representation of peripheral meridians. Single cases showed a movement of the center of gravity formed by a spatial maximum of population membrane potential. This movement travelled according to the stimulus representation site along the vertical meridian. However, this second representation did not move in accordance with the first one at the 17/18 border. In some cases both representations moved into the same direction, in others the representation at the 19/21 border moved into the opposite direction to the one in areas 17/18. In other cases the center of gravity showed no significant motion pattern.

3.2 Electrophysiology

3.2.1 Response detection at the initial stimulus representation site at the 17/18 border

When presenting a single moving or stationary white square in the center of visual field it evoked an increase of firing rate of the neurons at the border between visual areas 17 and 18. This spiking activity was detected and analyzed for the center electrode in five animals (1-4, 6, mean values calculated for each animal) (Table 10, 11). The center electrode was defined by the initial receptive field mapping and with additional receptive field mapping with all array electrodes in between sessions (Figure 21). Peri stimulus time histograms of multi unit activity recorded with the center electrode are shown in Figure 22 for the control and stimulus conditions.
Histology confirmed the placement of the electrode array at the 17/18 border in all cases. For animal 5 it was not possible to detect responses with manual or program-operated receptive field mapping during the experiment. The array electrode was placed at different positions with the aim of finding the vertical meridian. Later, histology showed that two penetrations were placed at the border between areas 17 and 18, one of which showed a program error in the output file. With this small

amount of data and without any map of the receptive fields it was not possible to determine the center electrode. For this reason results were not included in this analysis.

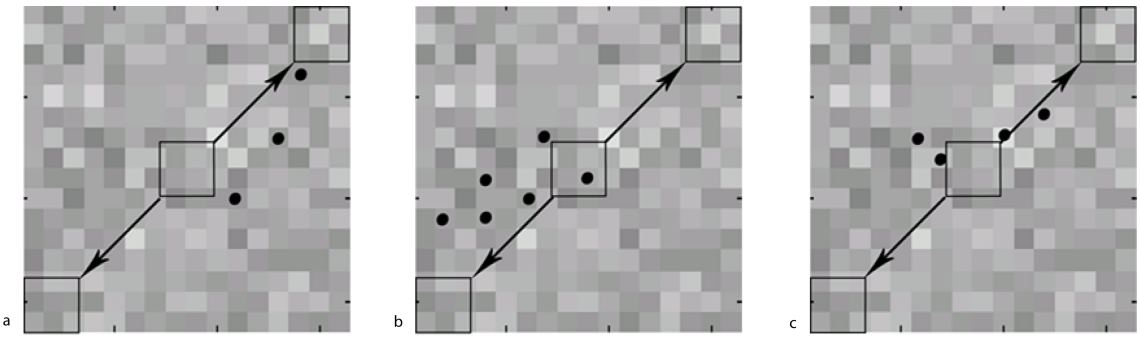

Figure 21: The receptive field mapping of the eight electrodes placed on the 17/18 border. A random dot chessboard pattern is shown to the animal as described in the methods section. The square that is used in the stimulus trial is superimposed to indicate how it is moved across the screen (arrows). Electrodes are placed at cortical positions that represent positions on the screen along the path the square travels. Note that the square and the motion path are not shown during the mapping. They are shown here for better understanding only. The center electrode is placed at the cortical site that represents the center of the screen in the visual field. The lateral electrodes are placed at the representation of the upper right part; the medial electrodes are placed at the representation of the lower left part of the screen. Now the receptive field mapper program is run for every electrode of the array. As a result the receptive field that is "viewed" by each investigated part of the cortex will be presented on the screen as described above. Each figure shows a mapping performed in a different animal (a: animal 3, b: animal 4, c: animal 6). Black dots indicate the center of the receptive field found by the program. It was not possible to get responses for all electrodes in any animal. However, the fields that could be determined all lie on the path the square takes when travelling across the screen. N.b.: The greyscale shown in the figure is random and does not display the actual receptive field status for any of the dots. It was used simply as a background to visualize the steps taken.

Table 10: Mean response onset latencies of significant responses (time in ms after response onset) in the remaining five animals at the electrode placed at the representation of the center of visual field at the 17/18 border

Animal	*Onset (Upwards)*	*Onset (Downwards)*	*Onset (Stationary)*
1	147	102	No significant onset
2	25	28	23
3	105	44	32
4	25	25	25
6	25	25	25
Average	64.4	44.7	26.3
Standard deviation	57.3	32.7	3.7

The significance of the difference between response onset latencies for the motion conditions as opposed to the stationary condition was tested with a two-tailed t-test. There was no statistically significant difference for response onset latency between the upwards moving square and the stationary square ($p=0.38$). Neither was there a statistically significant difference for response onset latency between the downwards moving square and the stationary square ($p=0.24$).

Table 11: Mean latencies to 90% peak firing rate at the initial representation site at the 17/18 border

Animal	*Latency(Upwards)*	*Latency (Downwards)*	*Latency (Stationary)*
1	147	270	299
2	34	37	29
3	74	38	95
4	39	22	25
6	72	92	37
Average	65.4	91.9	83
Standard deviation	57.4	103.2	86.4

The significance of the difference between latency to 90% peak firing for the motion conditions as opposed to the stationary condition was tested with a two-tailed t-test. There was no statistically significant difference in time to 90%peak firing between the upwards moving and the stationary square (p=0.56). Neither was there a statistically significant difference in time to 90% peak firing between the downwards moving and the stationary square (p=0.68).

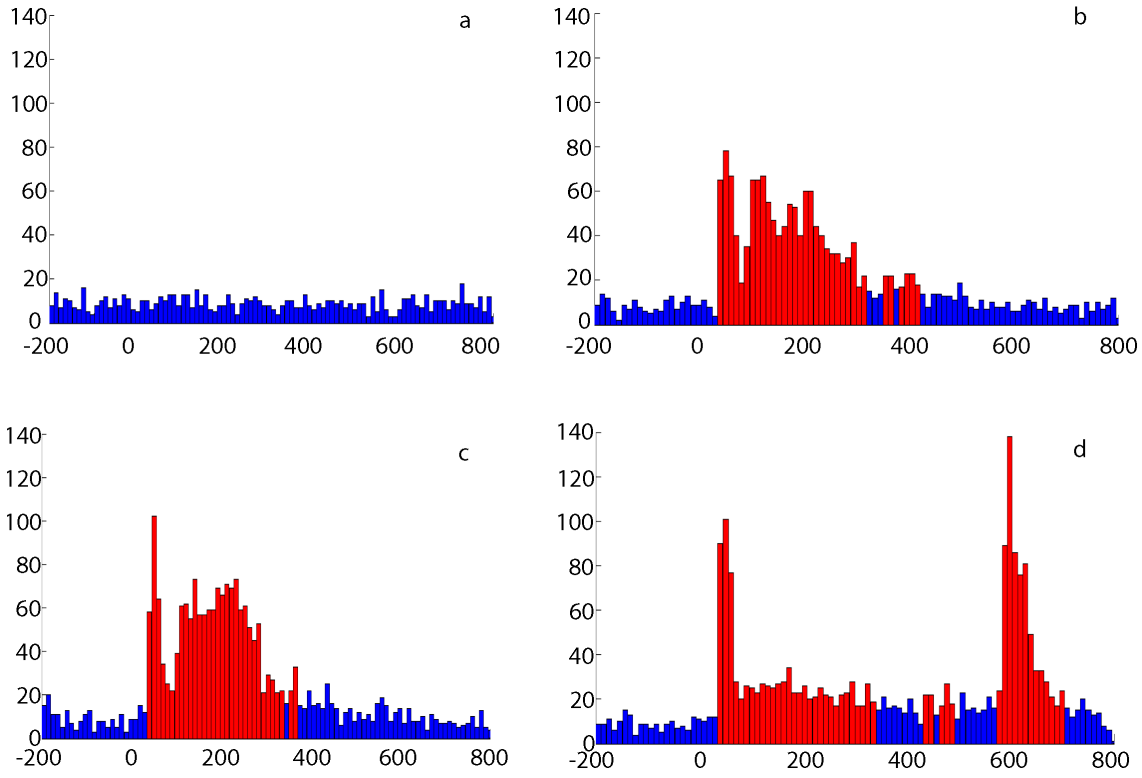

Figure 22: Peri-stimulus time histograms of multi unit activity recorded with the center electrode at the 17/18 border. This site represents the center of visual field. X-axis shows time in ms, y-axis spikes per 10ms bins. Stimulus onset at 0ms, stimulus offset at 550ms. a. Activity evoked by the blank condition. b-d. Activity evoked by the upwards moving (b), downwards moving (c) and stationary square (d).

3.2.2 Response detection of electrodes along the vertical meridian in areas 17/18

Again, data from animal 5 was not included in the analysis because it was not possible to determine the center electrode. Response latency at the electrode positions with increasing distance from the electrode placed at the initial representation site was investigated for the remaining five animals (mean values calculated for each animal). The significant responses showed the following onset latencies at the electrode penetration sites: The upwards moving square evoked significant firing onsets with latencies increasing with distance laterally from the center of representation in four out of five animals. For the electrodes placed medially to the center penetration the latency of significant onset increased towards the medial edge in all five animals. The downwards moving square evoked significant firing onsets with latency increasing with distance lateral from the center electrode in four out of five animals. At the electrodes placed medially to the center penetration the latency of significant firing onsets increased with distance from the electrode at the initial representation site in four out of five animals. Figure 23 shows an example of the visualization of the recorded spiking activity at the 17/18 border for the motion and stationary conditions.

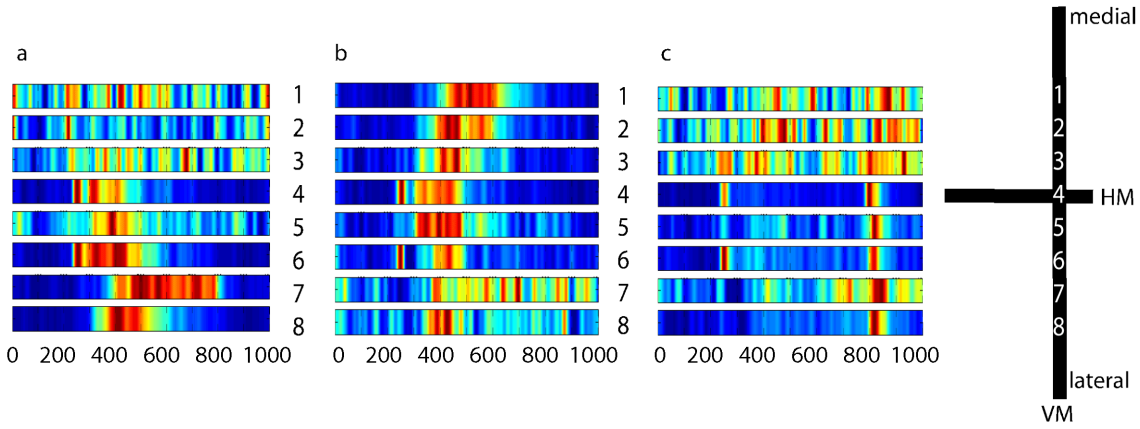

Figure 23: Spiking activity recorded at the 17/18 border in one animal. X-axis shows time in ms. Each of the eight traces shows multi unit activity recorded with one electrode during stimulus presentation. Electrodes are placed as displayed in the black cross on the right. HM: Horizontal Meridian, VM: Vertical Meridian. Thus, the upper trace shows the responses detected by the most medial electrode (1); the lowest trace shows the responses detected by the most lateral electrode (8). Electrode 4 is placed at the initial representation site. Each trace is normalized to 1 against itself (1 being displayed as red, 0 as blue). Stimulus on at 200ms, stimulus off at 750ms. a. Responses detected when presenting the upwards moving square. Cortical representation is located at subsequent positions lateral to the center. b. Responses detected when presenting the downwards moving square. Cortical representation is located at subsequent positions medial to the center. c. Responses detected when presenting the stationary square.

For the stationary square the latency of significant response onsets was calculated for all electrodes. At the electrodes placed lateral to the initial presentation site the latency of significant firing onset increased with distance from the center in three out of five animals, decreased in one and showed no subsequent latency differences across electrodes in one animal (Fig. 24). At the electrodes placed medial to the center representation site latency increased with distance from the center in four out of five animals and showed no latency difference in the fifth animal. The time to 90% peak response showed the following latencies across penetration sites: For the upwards moving square the latency to 90% peak increased with lateral distance from the center electrode in all five animals. At the penetrations placed medial to the center electrode latency increased with distance from the initial representation site in all five animals. For the downwards moving square the latency to 90% peak increased with lateral distance from the center electrode in four out of five animals and decreased in one animal. At the penetrations placed medial from the center electrode latency increased with distance from the initial representation site in all five animals. For the stationary square the latency to 90% peak increased with lateral distance from the initial representation site in all animals. Across the electrodes placed medial to the center electrode latency increased with distance from the initial representation site in three out of five animals and decreased in two.

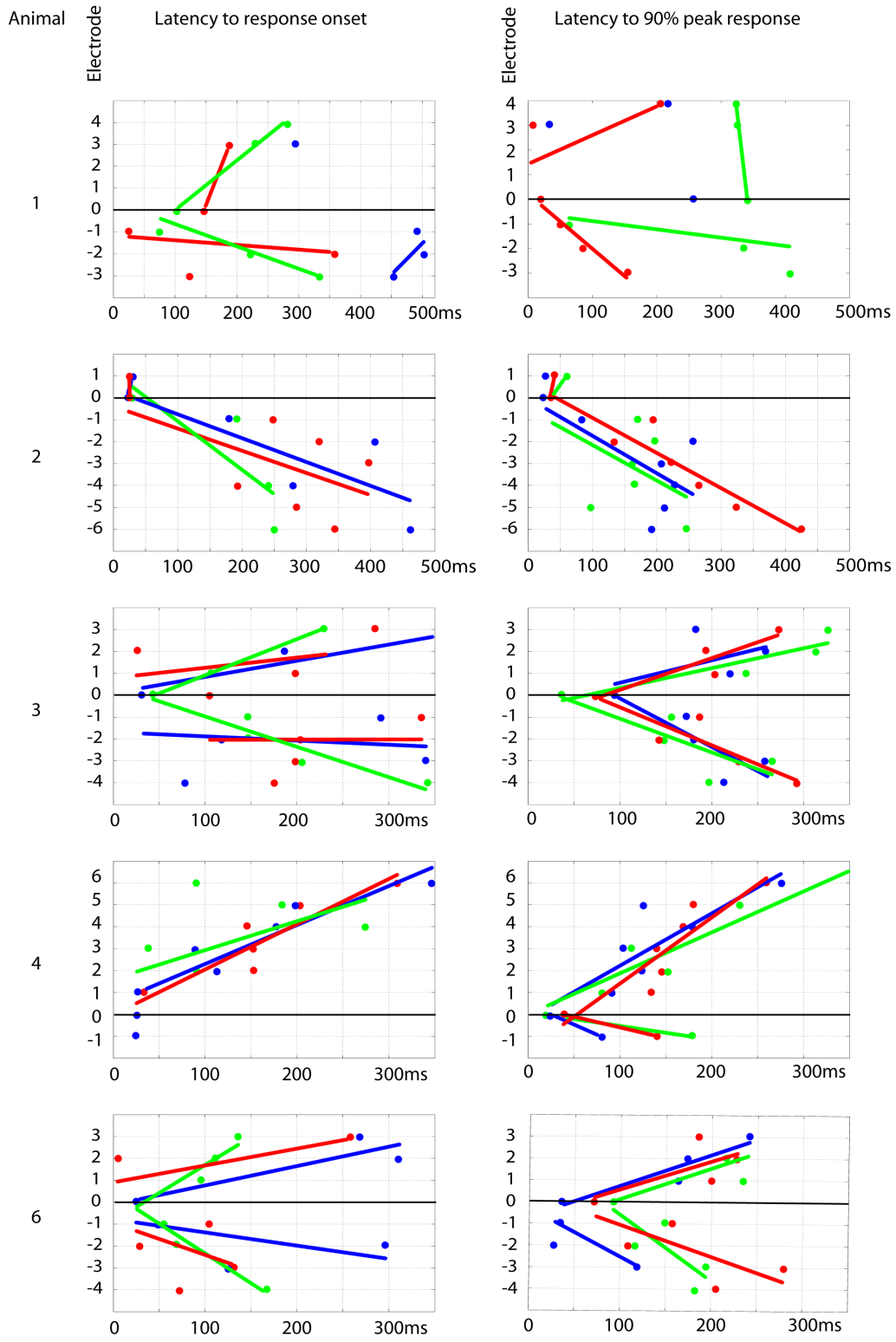

Figure 24: Timing properties of multi unit activity as response to all three conditions. The left column shows latency to response onset. The right column shows latency to 90% peak response. The x-axes show time in ms. On the y-axes electrode numbers are displayed. The electrode placed at the initial representation site is named "0". Electrodes with increasing distance from the center are given positive (medial placement) or negative (lateral placement) numbers. Each dot shows the onset -or 90% peak latency- timing for a single electrode. Red traces show response timing for the upwards moving square. Green traces show response timing for the downwards moving square. Blue traces show response timing for the stationary square.

However, when looking at the peri-stimulus time histograms (PSTHs) of the responses it becomes obvious, that the responses along the motion trajectory are stronger and more consistent in time than for the electrodes that lie outside the motion trajectory. Figure 25 shows an example for one animal with both motion conditions to visualize the difference between both situations.

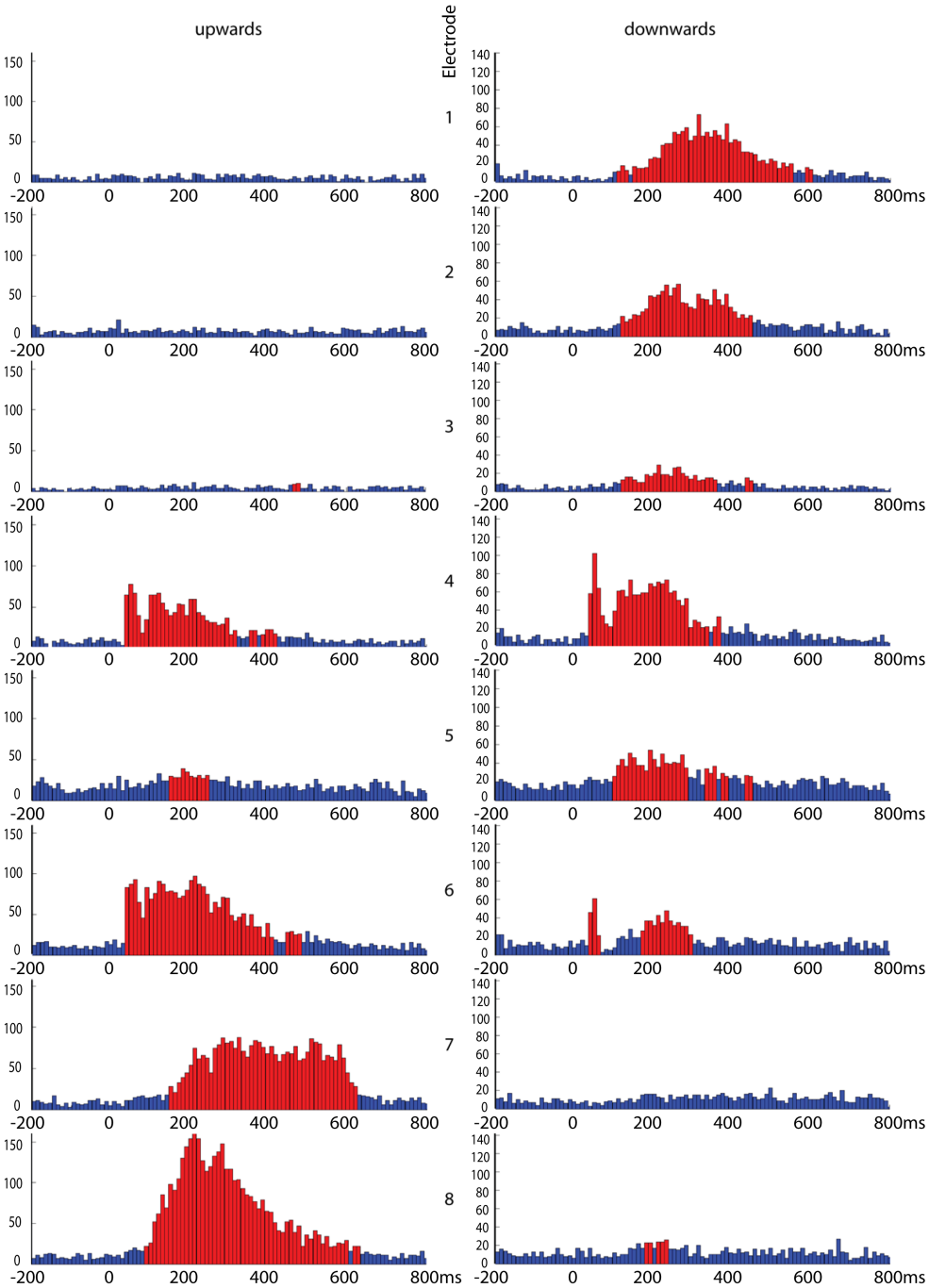

Figure 25: PSTHs of multi unit activity. X-axes show time in ms, y-axes show number of spikes per 10ms bin. Stimulus on at 0ms, stimulus off at 550ms. For each electrode placed on the 17/18 border (1-8) response patterns are shown: electrode 4 was placed at the initial representation site, electrodes 1-3 medial, electrodes 5-8 lateral. On the left side, PSTHs for the upwards moving square are shown (cortical representation at subsequent positions lateral to the placement of electrode 4). On the right side, PSTHs for the downwards moving square are shown (cortical representation at subsequent positions medial to the placement of electrode 4).

In addition to response onset and 90% peak latency timing at different electrodes a correlation analysis was performed for the electrodes of the array placed on the 17/18 border. Response patterns for all electrodes were correlated to the one at the center electrode. The time shift that resulted in the maximal possible correlation as well as the level of correlation was determined (Figure 26).

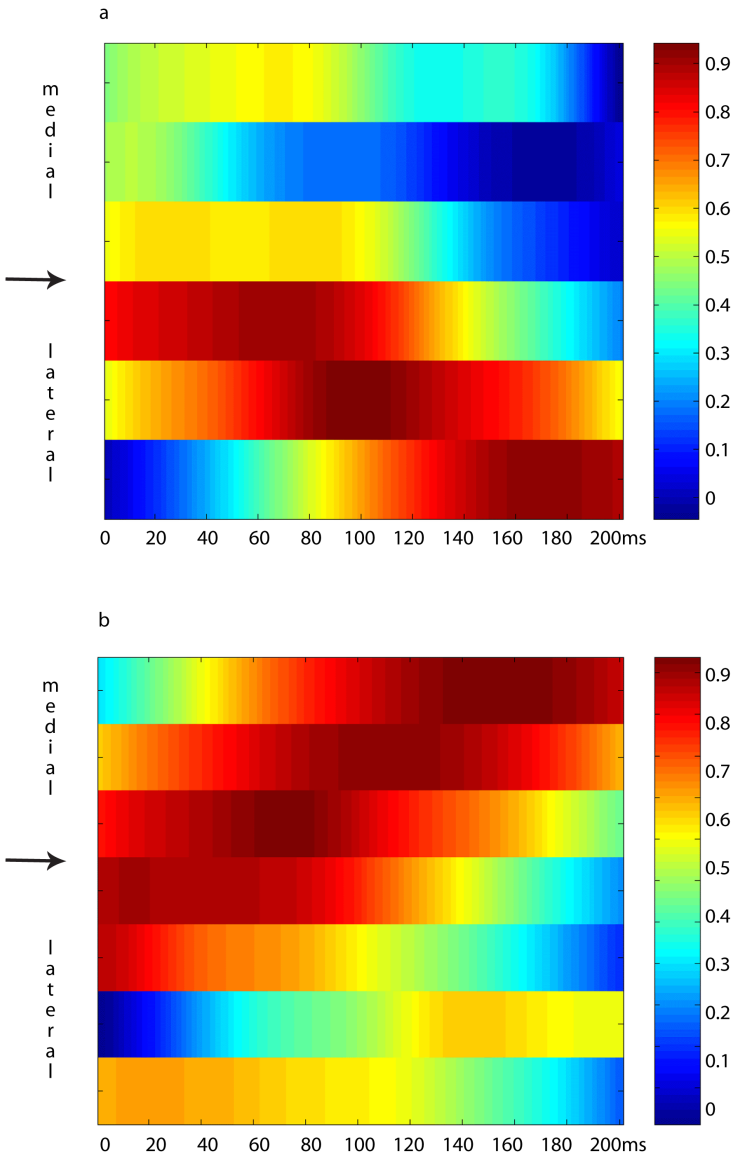

Figure 26: The result of a correlation analysis performed with the electrodes placed at the 17/18 border. In both a and b time is displayed on the x-axis. Each lead shows a correlation pattern for a single electrode. The electrode placed at the initial stimulus representation site serves as reference. The degree of correlation is colour-coded, red being the maximum possible degree of correlation. The time axis displays the amount of time necessary to shift the signal from two neighboured electrodes to receive the highest possible correlation of response patterns. Arrows indicate the placement of the center electrode. Medial positions are displayed in the upper half of both figures; lateral positions are displayed in the lower half. The maximum correlation is possible at positions lateral to the center electrode for the upwards moving square (shown here for animal 3) and at positions medial to the center electrode for the downwards moving square (shown for animal 6).

3.2.3 Response detection in higher order visual areas

In higher order visual areas 19 and 21 response onsets and 90% peak latencies could be detected for the majority of penetration sites in all six animals. However, no reproducible pattern of onsets of significant firing or latency to 90% peak was observed across animals. The positions of the earliest and latest activated area were different for all animals (Figure 27).

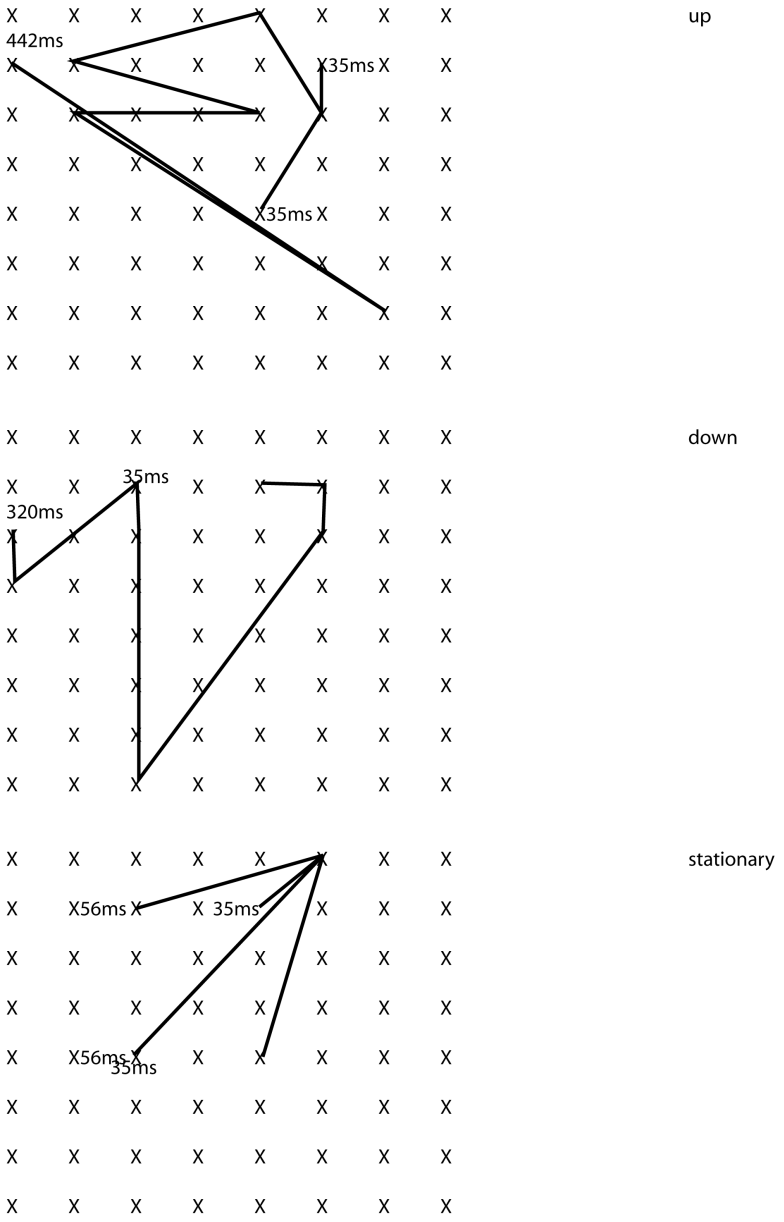

Figure 27: An example of electrodes detecting subsequent significant response onsets of multi unit activity in one animal. Each "X" marks one electrode; rows show penetrations (1-8), columns show electrodes on one array (1-8). Each part displays the response pattern for one condition. First significant response onset times are marked in ms. Then lines are drawn to the next electrodes that show significant response onsets with increasing latency. The last significant response onsets are again marked in ms.

3.3 Comparison of spiking activity and population membrane potentials

Both spiking activity and population membrane potentials show similar response onset latencies at the crossing of the horizontal and vertical meridian in areas 17/18. The significance of the difference between response onset latencies at the representation in areas 17/18 detected with electrophysiological recordings as opposed to the ones detected with Voltage Sensitive Dye Imaging was tested with a two-tailed t-test. There was no significant difference in onset timing of spiking activity as opposed to population membrane potentials for the upwards moving ($p=0.66$), the downwards moving ($p=0.52$) or the stationary square ($p=0.10$). The significance of the difference between latencies to 90% peak response at the 17/18 border detected with electrophysiological recordings as opposed to the ones detected with Voltage Sensitive Dye Imaging was calculated with a two-tailed t-test. There was no significant difference in latency to 90% peak response of spiking activity as opposed to population membrane potentials for the upwards moving ($p=0.15$) or the downwards moving square ($p=0.07$). The stationary square only showed 90% peak latencies of population membrane potentials in three animals, for one of which no electrophysiological data was acquired. Therefore no investigation of difference between 90% peak latencies for electrophysiological recording and Voltage Sensitive Dye Imaging was done.

4 Discussion

Stimuli moving through the visual field of an observer's fixed eye will result in image motion across the retina. Given the retinotopic organization of the visual cortex, it seems consequential to expect moving stimuli to move across the cortex accordingly. Investigating the cortical response behaviour to moving stimuli along a motion trajectory has not been done before. However, computation of moving stimuli has been investigated for many years. In the beginning of the 20th century psychophysicists started examining motion perception in human observers. Hubel and Wiesel (1959, 1962) pioneered electrophysiological recordings in the visual cortex by investigating direction selectivity of neurons in monkeys and cats. Investigating motion computation with Voltage Sensitive Dye has first been done by Grinvald et al. (1994) who examined the responses of the monkey visual cortex to moving gratings. In this study it was shown with two different methods in the visual cortex of the ferret how motion computation follows the retinotopic map across cortex.

4.1 Retinotopic mapping of stimuli in the center of visual field.

A contrast square was presented in the center of visual field of the anaesthetized ferret. This resulted in both increase of firing activity and population membrane potentials at the cortical stimulus representation site in visual areas 17 and 18. Furthermore, the population membrane potentials increased at the representation of the vertical meridian in areas 19/21. The detected representation sites were in accordance to the retinotopical organization of ferret visual areas 17, 18, 19 and 21 (Manger et al., 2002). The increase of population membrane potentials at the band between the two initial representation sites as well as the increase of population membrane potentials and multi unit activity along the vertical meridian at the 17/18 border was as expected due to lateral connections within and across these areas (Manger et al.; 2002, Roland, 2002).

4.2 Response onset timings for different conditions

Response onset latencies of spike trains showed a relatively wide range across animals with an average of 64.4ms (upwards moving square), 44.7ms (downwards moving square) and 26.3ms (stationary square). The rather high value for response onset time for the upwards moving square as compared to the downwards moving square and the stationary square is mostly caused by the responses detected in animal 1 (147ms). Obviously, these 147 ms are due to noise, or a poor signal, or some error in our measurement. In this animal responses were only detected for one out of six penetrations (conditions two and three), for the other penetrations no responses could be detected at all. The stationary condition did not evoke any responses. Therefore these values are not mean values calculated across several penetrations. This might be the reason for the late response onset as opposed to other experiments.

Excluding this animal leads to a mean response onset time of 45ms after stimulus onset. The literature contains no information about spike response onset latency of multi units to visual stimuli in area 17 of the ferret. Usrey et al. (2003) investigated latencies to peak response for single units of area 17 in the ferret after stimulation with a 100% contrast receptive field mapper stimulus with varying frequency. Time to peak for simple cells was 65ms, for cells with complex receptive fields it was 44ms in the center and 48ms in the surround. Response onset latencies to moving grating visual stimuli in cat V1 have been detected with single unit recordings after a mean latency of 84ms (Ouellette & Casanova, 2006). The fibers of the optical tract and optical radiation are shorter in the ferret than in the cat. This might explain the lower latency to response onset detected in the ferret. However, fibers might show a different thickness and thereby conduction velocity. Therefore at this point it is not possible to compare our results in quantative terms to the ones that can be found in the literature.

The fact that the stationary square evoked responses as fast as (or even faster than) the movement conditions (neither spiking activity nor population membrane potential showed earlier onset in response timing for moving as opposed to stationary stimuli) seems surprising and is not in accordance with the literature. The following considerations can be made: By the time the initial response onset reaches the visual cortex the image has already moved on the retina. However, moving objects are not perceived behind their actual position. I.e. it is possible for an observer to predict a moving object's location along a motion trajectory. Motion processing pathways are activated by changes of image position on the retina over time. Since the main delay for the processing of all visual stimuli occurs in the retina, retinal ganglion cells are considered to compensate for the large delay by anticipating future positions of a stimulus moving with constant velocity (Berry et al., 1999). Therefore, it might be possible that during the delay in the retina succeeding the initial activation motion pathways are already activated by the moving stimulus leading to activation of expected subsequent retinal positions. Furthermore, pathways of the optic nerve, tract and radiation are expected to operate faster than pathways computing stationary stimuli in monkeys (Livingstone & Hubel, 1988; Bullier, 2001) and in cats (Jancke et al., 2004). Neurons computing motion pathways have thicker axons and stronger myelination. Therefore they can forward signals faster than pathways computing stationary stimuli that show a poorer myelination (Bullier, 2001). As a consequence, motion pathways can detect the image at several subsequent positions on the retina and forward the initial onset as well as a motion signal to the cortex even faster than the pathways computing stationary stimuli can send the information about stimulus onset. Onset latencies of population membrane potential tended to be longer for the stationary condition than for the motion conditions. The mean response onsets were evoked after a latency of 32ms (upwards moving square), 38ms (downwards moving square), 59ms (stationary square), respectively. First mean response onsets were de-

tected after 23ms (upwards moving square) and 20ms (downwards moving square) as opposed to 33ms for the stationary square. However, with data from six experiments and a rather large variance of onset timings this difference is not statistically significant. Thus, at this point the data does not support the notion of a difference of response onset timing for stationary as opposed to moving squares at the initial retinotopic site in ferret visual areas 17/18. Investigating the time to response peak of both spiking activity and network membrane potential leads to a similar result. Mean time to 90% peak firing of multi units was 65ms (upwards moving square), 92ms (downwards moving square) and 83ms (stationary square). Again, the motion did not evoke faster peaking responses than the stationary condition, as opposed to what one might expect. The earliest peaks were detected after 34ms (upwards moving square), 22ms (downwards moving square) and 25ms (stationary square). Due to the lack of significant peak of population membrane potentials in three animals (see table 5) the latency differences for motion as opposed to stationary conditions were not determined (see results section). First peaks were detected after 59ms (upwards moving square), 58ms (downwards moving square) and 70ms (stationary square). Computation of continuously moving objects in the visual cortex of the ferret has not been investigated yet. With sparse information from the literature and the rather small number of animals used in this study it cannot be explained why the common knowledge about motion computation could not be confirmed.

4.3 Response onset with different methods

Most afferent fibers from the LGN project to lamina IV of V1 (Hendrickson et al., 1978; Diamond et al., 1985; Sincich & Horton, 2005). From lamina IV signals are forwarded to supra- and infragranular laminae (Lund, 1988). Voltage Sensitive Dye Imaging gives information about changes in population membrane potentials in lamiae I to III mostly (Grinvald & Hildesheim, 2004). Since lamina IV neurons receive direct input from the LGN (Hendrickson et al.; 1978, Diamond et al., 1985; Sincich & Horton, 2005) and then forward signals to supra- and infragranular laminae (Sincich & Horton, 2005; Roland 2006) one would expect response onsets in laminae I-III to show longer latencies than those of action potentials in lamina IV. The present data provided some evidence that for the two motion conditions latency to response onset was shorter for VSDI as opposed to electrophysiological recordings. For the stationary stimulus the mean response onset tended to be shorter for electrophysiological recordings. However, all these latency differences show no statistical significance. 90% peak latency was higher for all conditions with VSDI than with electrophysiology but, again, showed no significance for the upwards or the downwards moving square. For the stationary square no t-test was performed since there was only significant data for three animals.
It was not possible to reconstruct the exact depth of the electrophysiological recording sites after the experiments. Recording action potentials from lamina IV would

lead to earlier response onsets than recording with Voltage Sensitive Dye. Assuming that action potentials were recorded from supra- or infragranular laminae the initial thalamic input to lamina IV would not have been detected. Thus, recording action potentials in supra- or infragranular laminae might very well occur with latencies similar to the population membrane potentials detected with Voltage Sensitive Dye.

4.4 Feed forward activity

The responses of population membrane potentials showed two representations of the stimulus, one in primary visual cortex (area 17) and area 18 and one in higher order areas 19 and 21. In the presented experiments, the second representation appeared later than the first one. This finding was, however, only statistically significant for the upwards moving square. Assuming a hierarchical organization of cortical areas one might expect a stimulus representation in higher order areas to be activated due to feed forward input from lower order areas (Maunsell & van Essen, 1983). I.e. the second representation site would show an increase of activity subsequent to the first one. However, the strict hierarchical model of processing in the visual cortex seems to be obsolete. Schroeder et al. (1998) described in the monkey brain that moving visual stimuli excite higher order areas sensitive to motion with latencies similar to those detected in V1. Hence responses to motion stimuli in higher order visual areas can very well appear with latencies similar to those in V1 (Bullier, 2001). Such data can be explained as follows: First, as mentioned above, fibers conducting motion signals operate very fast. By the time the input information about a stationary square reaches V1, the information about a moving stimulus has already been forwarded to higher order areas. All signals are transduced through V1, but for motion stimuli they reach higher order areas with similar latencies. Second, in the cat, Khayat et al. (2000) have shown that there are fibers conducting motion signals that go directly from the LGN to area 19. It can be assumed that these fibers also exist in the ferret, leading to a fast signal transduction to higher order visual areas. Finally, the VSD signal shows changes in activity in laminae I to III. Since the initial input in V1 arrives in lamina IV it will take some time for the activity to be forwarded to more superficial laminae and be detected as a VSD signal. By this time the signal has already been forwarded to higher order areas and causes an increase of activity there. More experiments would have to be done to further explore the population dynamics and to more accurately map spiking activity in higher order visual areas.

4.5 Motion in areas 17/18

Investigating the onset latencies in areas 17 and 18 with increasing distance from the initial representation site clearly showed a motion pattern across animals. This was seen for both spiking activity and population membrane potentials. Given the retinotopic mapping of azimuths and elevations to the visual cortex (Manger et al.,

2002) this is what was expected along the motion trajectory of the stimulus. When investigating the speed of the moving representation site in the VSD signal two things became obvious: (i) When detecting the arrivals of peak depolarization at the subsequent representation sites latencies increased with distance from the center representation. The fact that, for the upwards moving square, two out of six animals appeared to show a motion pattern from the periphery to the center was probably due to inaccurate centering of the monitor to the initial representation site. (ii) Calculating the velocity of this spread of activity along the subsequent representation sites of the moving stimulus resulted in velocities similar to the one of the stimulus. This held for both upwards and downwards moving squares. Since the monitor was placed 57cm in front of the animals' eye we knew that one cm of the viewed area corresponded to one degree of visual angle (Manger et al., 2002). One mm on the ferret cortex along the vertical meridian in areas 17/18 corresponds to five degrees of visual angle (Manger et al., 2002). Manger's map of the ferret cortex (Manger et al., 2002) was used to determine the velocity of the stimulus representation with the data calculated from the subsequent array channels along the motion trajectory. The results showed an average movement with 27 °/s for the upwards moving square and 38°/s for the downwards moving square. The stimulus moved with a velocity of 24°/s. The discrepancy between expected and calculated velocity can be explained as follows: the map was created using a flattened ferret brain. Therefore, the distances between cortical points will be larger than the ones covered with the array in vivo. Thus, when using this map, velocities will appear greater than they actually are. It was not possible to exactly determine the deviation for an individual ferret brain. Furthermore, the map shows centres of visual fields of neurons lying exactly on the vertical meridian. Potentially our stimulation might have been slightly off the vertical meridian, stimulating cells with different receptive field characteristics and different elevation representations.

The subsequent increase of response latencies was also found for the electrophysiological recordings. However, by investigating response onset latencies it was not possible to determine the direction of the stimulus motion. Subsequent latencies of response onset were found with electrodes placed at both sides of the initial stimulus representation site. To determine the difference in responses evoked along the motion trajectory as opposed to the other side, PSTHs were investigated. These showed a more constant and stable pattern for the responses recorded along the representation of the motion trajectory. Furthermore, the correlation of response patterns across the electrodes of the array showed a higher level of correlation at the electrodes placed along the subsequent stimulus representation sites than for the opposite side. Also a more consistent time shift between different electrodes was seen for the electrodes placed along the representation of the motion trajectory. These two methods showed that, although neurons respond to the moving stimulus in both directions, the pattern is a different one along the motion trajectory than

at the other side of the array. The fact that the visual cortex was responding to the stimulus even at positions outside the representation site might be due to both intrinsic activity and lateral spreading depolarization within areas 17 and 18 (Grinvald et al., 1994; Lamme et al., 2000; Roland et al., 2006). Also, activity at stimulus representation sites showed higher amplitude than activity at positions corresponding to the background. Since receptive fields of neurons in V1 overlap a population receptive field is activated in response to a visual stimulus; neurons with receptive fields in the center of stimulus representations show higher activity than neurons with more peripheral receptive fields (Jancke et al., 2004). Thus, it is very possible that the activity of complex networks of neurons rather than recording errors or imprecise reconstruction lead to the recording of signals at cortical positions outside the stimulus representation site.

The receptive field mapper program did not provide a receptive field for every unit that was recorded from, i.e. for some penetration sites no receptive field was found. Therefore, there is not enough data to know precisely at which time point which part of cortex was activated by which position of the stimulus on the screen. Also, since the ferret's head was tilted by 45°, the stimulus was viewed as a rotated square with a maximum medio-lateral extension mapped to 1mm of cortex. Since electrode spacing was 400μm it is possible that two electrodes picked up a response onset to the stimulus simultaneously. Furthermore, the square might not have been presented exactly on the vertical meridian and one corner of the square might have been mapped exactly between two electrode penetration sites, thereby activating none of the recorded units at stimulus onset. Also the electrodes of the array most likely recorded signals from different layers of cortex, which makes it difficult to compare response onset latencies. Therefore, unlike for the VSDI, subsequent onset latencies across the representation sites of the motion trajectory were not calculated and no estimate of response onset velocity was made.

Geisler (1999) and Jancke (2000) described a "motion streak", a continuous smear of activity along the trajectory of a moving stimulus. This streak is said to be used to extract information about orientation of the motion trajectory but conceal the actual location of the stimulus at subsequent positions. Our data do not support this view. With both Voltage Sensitive Dye Imaging and electrophysiological recordings at several positions along the motion trajectory subsequent on- and offset of responses were detected at the stimulus representations sites along the motion trajectory.

4.6 Motion in areas 19/21

Population membrane potentials at the 19/21 border showed an increase of activity as in areas 17/18. In some cases this second representation was moving along with the first one. This was expected according to the retinotopic organization in areas

19 and 21 (Manger et al., 2002). However, the motion of the stimulus representation site was not as consistent as in areas 17 and 18. Since in one animal the vertical meridian of areas 19 and 21 was outside the imaged area, there is only data from five animals. The second representation site showed motion along the motion trajectory, in accordance with the one in 17/18 as shown in the velocity calculation. However, in many cases the representation did not move along with the one in 17/18. The less consistent motion pattern in 19/21 can be explained as follows: First, these areas do not receive direct input from the thalamus like area 17. Input comes from lower, striate and extrastriate areas (Roland et al., 2006). Each area holds a representation of the visual field but they still show some differences: Receptive field size of neurons increases from area 17 to 21 (Manger et al., 2002) so the neurons in higher order areas are not as accurate computing items in their visual field as earlier areas. Second, the horizontal meridian shows a dual representation in area 21, but not in area 19 (Manger et al., 2002). A dual representation results in a broader area of representation at the 19/21 border that splits into two in area 21, i.e. in area 21 elevations above the zero meridian are mapped to the part between the two representations and lateral to the more lateral one. Elevations below zero degrees are mapped to areas medial to the medial representation of the vertical meridian (Manger et al., 2002). The differences in receptive field size and the dual representation might explain why it is more difficult to detect motion along the vertical meridian in areas 19 and 21 than in areas 17 and 18.

4.7 Future prospects

The results of the present study suggest designs for some additional experiments, and provide a basis to the improvement of the methods of multi unit recording and VSD imaging.

4.7.1 Additional experiments

For future experiments it would be interesting to investigate responses to the stimuli in the same areas (areas 17, 18, 19 and 21) in more animals to study population membrane potentials more thoroughly. In addition it would be important to obtain a more accurate mapping of spiking activity in areas 19 and 21. Furthermore, the feed forward input from area 17 to higher order areas could be investigated more closely in order to understand if there is really a higher latency to response onset at the vertical meridian in 19/21 as opposed to 17 and 18. The recording sites for both spiking activity and network membrane potentials could be extended to the posterior suprasylvian area. This area lies anteriorly adjacent to area 21 (Philipp et al., 2006; Cantone et al., 2006), and is expected to receive input from lower order areas especially in response to moving visual stimuli. It is a motion sensitive area in the ferret visual cortex, comparable to monkey area MT or cat PMLS (Philipp et. al. 2006). In the present study spiking activity was recorded from one depth

during each electrophysiological recording session. Recording from different layers with the electrode arrays would allow a more accurate exploration of activity in different depths of cortex in response to the moving and stationary stimuli.

4.7.2 Improvement of multi unit recordings

Since penetration of the cortex with electrodes influences the distribution of VSD during the staining process it was not possible to perform an extended receptive field mapping at the 17/18 border prior to VSD imaging. Therefore, the initial receptive field mapping was only done at one position, selected with the help of anatomical landmarks. However, a more accurate initial mapping of receptive fields in both areas 17/18 and 19/21 before the VSD imaging would be useful. Thereby the stimulation could be adjusted to the center of visual field more precisely and the initial presentation of the stimulus mapped exactly to the crossing of the two meridians. Furthermore, when recording with arrays of more than one electrode the vessels on the cortical surface restrict the potential penetration sites. In theory it would be interesting to use electrodes that allow closer spacing and also more leeds to cover a bigger area. That is, however, very difficult to realize in practice without penetrating vessels. The next limitation is the bent shape of the cortical surface. Therefore, when using an array with electrode tips aligned, the electrodes will record signals from different cortical depths. Since every brain is different and the same arrays were used in many different positions on cortex this problem cannot be easily overcome. By passing current through the electrodes at the end of the experiments coagulation marks can be left in the tissue. These marks can then be used after sectioning to reconstruct penetration sites and obtain information about penetration depth. In our experiments we made an attempt to leave coagulation marks. However, we were not able to see all marks during histological evaluation. Therefore, for future experiments, the amount of current as well as the coagulation time could be increased to more clearly show the positions of the recording electrodes.

4.7.3 Improvement of VSD imaging

Due to the dense arrangement of cortical cells and penetration properties of the dye molecules the strength of the fluorescence signal decreases with cortical depth. Therefore, the Voltage Sensitive Dye signal mostly gives information about activity in the upper cortical layers (Grinvald & Hildesheim, 2004). It would be interesting to image the deep cortical layers and to compare the signals to electrophysiological recordings. Another issue is the low signal-to-noise ratio of the VSD signal (Shoham et al., 1999). Pulsation artefacts due to heartbeat and respiration make it necessary to use subtraction and averaging methods (Shoham et al., 1999). Thus, many trials have to be recorded to be able to perform a statistic analysis on the data. However, due to dye bleaching with light exposure data acquisition time is limited. Using dyes that allow for longer light exposure would increase the amount of data and give a

better base for analysis. Another problem, caused by the setup, is that the animal has to be moved under the camera for the VSD recordings and back out for the electrophysiology recordings. The screen has to be moved accordingly. Thus, there can be minor changes in the position of the animal's head relative to the screen. A setup that allowed for VSD imaging and electrophysiological recordings at the same position would eliminate these changes.

5 Abstract

Computations of Object Motion in the Visual Cortex of the Ferret
Sarah Wehner, Karolinska Institutet, Stockholm, Sweden

Introduction

For living in a world in motion it is of fundamental importance to perceive and process motion of objects and even predict their position along a motion trajectory. The image of the stimulus will move across the retina when viewing a moving stimulus with eyes fixed. Since the visual cortex is retinotopically organized the cortical representations can be expected to move accordingly. Although this statement seems consequential, it has not been tested experimentally before.

Methods

In this study we investigated the population membrane potential and spiking activity of the neurons in the visual cortex of six adult female ferrets (Mustela putorius) in response to natural stimulation. Up- and downwards moving white squares of 3.8° by 3.8° on a random dot background (48% contrast) were presented to the anaesthetized animal on a computer screen. A stationary white square served as control. Visual Ares 17, 18, 19 and 21 were stained with a Voltage Sensitive Dye (VSD) and imaged with a photodiode array camera. Multi unit activity was recorded with electrode arrays in the same areas. After the experiments the brains were sectioned and stained for cell bodies and cytochrome oxidase to reconstruct area borders. Responses to visual stimuli in the VSD and electrophysiology signal were processed with Matlab®to investigate network membrane potentials and spike trains.

Results

When presenting a contrast square at the center of visual field it was mapped to the crossing of the vertical and horizontal meridian in areas 17/18. This resulted in changes of both population membrane potential and spiking activity. When recording electrophysiologically and with Voltage Sensitive Dye at the initial locus -which matches the initial position in the visual field- the response onset timing showed no significant difference for stationary as opposed to up- or downwards moving stimuli. Neither did the response onset timing of the population membrane potential at the initial locus differ from that of the multi unit activity. The VSD recordings showed a second stimulus representation site at the crossing of the vertical and horizontal meridian at the 19/21 border. The response onset for the population membrane potentials at the second representation site was significantly later than at the 17/18-border for the upwards-moving square ($p<0.05$) but not for the downwards mov-

ing (p=0.07) or the stationary square (p=0.19). Due to sparse firing of the multi units in higher order areas the second representation could not be detected electrophysiologically. Population membrane potential and multi unit activity showed a successive increase of response onset latencies along the cortical representation of the motion trajectory in areas 17 and 18. Onset latency increased at positions medial to the initial representation for downwards moving stimuli and lateral to the initial representation for upwards moving stimuli. A successive increase of response onset latencies of population membrane potential along the motion trajectory at the 19/21 border was seen for the upwards moving (three animals) and downwards moving square (one animal). However, this second representation appeared not to move in accordance with the first one.

Discussion

As expected from the retinotopic organization of areas 17, 18, 19 and 21 (Manger et al, 2002) a representation of stimuli presented in the center of visual field appeared at the 17/18 and 19/21 border. The lack of latency difference for response onsets to moving and stationary stimuli was unexpected, given the fact that motion pathways are thought to operate faster than those that compute stationary stimuli (Livingstone and Hubel, 1988). More experiments would have to be done to allow a more detailed analysis of onset latencies. Since VSD imaging gives information about population membrane potentials in layers I to III only (Grinvald and Hildesheim, 2004) one would expect response onsets to show longer latencies than those of action potentials due to synaptic input to layer IV neurons. It was not possible to reconstruct the exact depth of the electrophysiological recording sites after the experiments so no definite statement can be made about the origin of the spiking activity. Action potentials in supra- or infragranular layers might very well occur with latencies similar to the population membrane potentials in layer I to III. Given the anatomical connections of the visual system one might expect the latency for the response onset in areas 19 and 21 to be higher than for areas 17 and 18 for all conditions. However, the strict hierarchical model of processing in the visual cortex seems to be obsolete. In a study by Schroeder et al. (1998) it has been described in the monkey that moving stimuli excite higher order areas sensitive to motion with latencies similar to those detected in V1. More experiments would have to be done to further explore the population dynamics and to more accurately map spiking activity in higher order areas. The subsequent increase of response latency at recording positions along the motion trajectory in areas 17/18 for both spiking activity and network membrane potential was as expected given the retinotopic organization of the visual cortex (Manger et al., 2002). A moving representation at the 19/21 was expected in accordance with the one in areas 17/18. The fact that it was less obvious might be due to the later stage of processing and the larger receptive fields of neurons in higher order areas. It would be interesting to extend the

recording sites for both spiking activity and network membrane potentials to the posterior suprasylvian area that is said to be a motion sensitive area in the ferret visual cortex (Philip et al., 2006).

6 Deutsches Abstract

Computations of Object Motion in the Visual Cortex of the Ferret
Berechnung von Objektbewegung im visuellen Kortex des Frettchens
Sarah Wehner, Karolinska Institutet, Stockholm, Schweden

Einleitung

Für das Leben in einer sich bewegenden Umwelt ist es von elementarer Bedeutung, die Bewegung von visuellen Stimuli wahrzunehmen und zu verarbeiten sowie deren zukünftige Position vorherzusagen. Wird ein bewegter Stimulus mit fixiertem Auge wahrgenommen, so bewegt sich das Abbild des Stimulus auf der Retina des Betrachters. Aufgrund der retinotopen Organisation des visuellen Kortex kann man vermuten, dass auch die kortikale Repräsentation des Stimulus sich entsprechend dieser Bewegung verändert. Obwohl dieses Phänomen logisch scheint, wurde es bisher nicht experimentell verifiziert.

Material und Methoden

Die vorliegende Arbeit beschäftigt sich mit der Untersuchung von Summenmembranpotentialen von Neuronenpopulationen sowie Aktionspotentialen von "Multi Units" im visuellen Kortex von sechs erwachsenen weiblichen Frettchen (Mustela putorius) bei natürlicher Stimulation. Den anästhesierten Tieren wurden auf einem Computer-Bildschirm weiße Quadrate (3,8° x 3,8°) präsentiert, die sich vor einem ”random dot”-Hintergrund aufwärts, bzw. abwärts bewegten. Ein stationäres weißes Quadrat diente als Kontrollbedingung. Die visuellen kortikalen Areae 17, 18, 19 und 21 wurden mit einer spannungssensitiven Farbe (Voltage Sensitive Dye, VSD) markiert und mit einer Photodioden-Kamera abgebildet. In den selben Areae erfolgte die Ableitung von Multi Unit Aktivität mit Elektrodenarrays. Nach den Experimenten wurden die Gehirne der Tiere entnommen und histologisch aufgearbeitet (Dünnschnitte). Nach Färbung alternierender Schnitte nach Nissl-Substanz und Cytochrom-Oxidase erfolgte die Rekonstruktion der anatomischen Grenzen zwischen den Areae.

Ergebnisse

Ein durch Helligkeitskontrast definiertes Quadrat, das im Zentrum des visuellen Feldes präsentiert wurde, wurde an der Kreuzung zwischen horizontalem und vertikalem Meridian an der Grenze zwischen Area 17 und 18 abgebildet. Dies bewirkte sowohl eine Veränderung von Summenmembranpotentialen als auch die Auslösung von Aktionspotentialen. Bei der Ableitung von Signalen mit Elektroden und mit VSD an der initialen Repräsentationsstelle im Zentrum des visuellen Feldes zeigte

sich kein Unterschied in der Antwortlatenz zwischen bewegten oder stationären Stimuli. Auch zeigte sich keine Latenzdifferenz zwischen der Änderung des Summenmembranpotentials und der Multi Unit Aktivität. Die VSD-Ableitungen zeigten einen zweiten Repräsentationsort des Stimulus an der Kreuzung zwischen vertikalem und horizontalem Meridian an der Grenze der Areae 19 und 21. Die Membranpotentialänderung der untersuchten Neuronenpopulation an diesem zweiten Ort ereignete sich signifikant später als an der Grenze der Areae 17 und 18, jedoch nur für das sich aufwärts bewegende Quadrat ($p<0,05$) und nicht für das sich abwärts bewegende ($p=0,07$) oder das stationäre Quadrat ($p=0,19$). Aufgrund begrenzter Signale der Multi Units in den höheren Areae konnte der zweite Repräsentationsort elektrophysiologisch nicht weitergehend untersucht werden. Die Summenmembranpotentiale und Multi Unit Aktivität zeigten einen sukzessiven Anstieg der Antwortlatenz medial des initialen Locus für die sich abwärts bewegenden Stimuli sowie lateral für die Aufwärtsrichtung. Ein sukzessiver Latenzanstieg für die Summenmembranpotentialänderung entlang der Bewegungsbahn auf der Grenze der Areae 19 und 21 konnte für das sich aufwärts bewegende Quadrat (drei Tiere) und das abwärts bewegte Quadrat (ein Tier) gezeigt werden. Hierbei erfolgte jedoch die Bewegung dieser zweiten Repräsentation nicht übereinstimmend mit der ersten.

Diskussion

Entsprechend der retinotopen Organisation der visuellen Areae 17, 18, 19 und 21 (Manger et al., 2002) war die Repräsentation eines im Zentrum des visuellen Feldes dargestellten Stimulus auf der Grenze der Areae 17/18 sowie 19/21. Das Fehlen einer Antwortlatenz-Differenz für den Signalbeginn zwischen bewegten und stationären Stimuli war unerwartet, da Bewegungsbahnen schneller operieren als solche, die stationäre Stimuli verarbeiten (Livingstone & Hubel, 1988). Für eine tiefergehende Analyse der Latenzen wären weitere Experimente nötig. Da die Ableitung mit VSD vor allem Signale aus den kortikalen Laminae I bis III erfasst (Grinwald & Hildesheim, 2004), ist zu erwarten, dass der Antwortbeginn längere Latenzen aufweist, als die Ableitung von Aktionspotentialen an ihrem Entstehungsort in Lamina IV. Eine exakte Rekonstruktion der Penetrationstiefe der Elektroden nach den Experimenten war nicht möglich, daher kann keine definitive Aussage über den Ursprung der abgeleiteten Aktionspotentiale getroffen werden. Aktionspotentiale aus den supra- oder infragranulären Laminae (I-III bzw. V-VI) können mit ähnlichen Latenzen abgeleitet werden wie die Membranpotentiale mit VSD. Die anatomischen Verbindungen im visuellen System lassen eine längere Latenz bis zum Antwortsignal in Area 19 und 21 im Gegensatz zu Area 17 und 18 erwarten. Allerdings ist das strikt hierarchische Modell der Signalprozessierung im visuellen Kortex obsolet. In einer Studie von Schroeder et. al (1998) wurde beim Makaken gezeigt, dass bewegte Stimuli höhere bewegungssensitive Areae mit der gleichen Latenz erreichen wie V1. Weitere Experimente sind nötig, um die Dynamik der Neuronenpopu-

lationen zu untersuchen und die Aktionspotentiale in den höheren Areae genauer zu kartieren. Der kontinuierliche Anstieg von Antwortlatenzen an Ableitungsloci entlang der Bewegungsbahn an der 17/18-Grenze entsprach sowohl für Summenmembranpotentiale als auch für Aktionspotentiale den Erwartungen gemäß der in der Literatur beschriebenen retinotopen Organisation des visuellen Kortex (Manger at al., 2002). Eine Repräsentation sich bewegender Stimuli an der 19/21-Grenze wurde entsprechend der Bewegung auf der 17/18-Grenze erwartet. Die Tatsache, dass die Bewegung an der Grenze 19/21 weniger offensichtlich war, könnte durch die höhere Prozessierungsphase und die grösseren rezeptiven Felder der Neuronen in höheren Areae bedingt sein. Interessant wäre hier die Ausdehnung der Ableitungen von Membran- und Aktionspotentialen auf die Suprasylvischen Areae, die im Kortex des Frettchens als bewegungssensitive Regionen bekannt sind (Philip et al., 2006).

7 References

Arieli, A., Shoham, D., Hildesheim, R. & Grinvald, A. Coherent spatiotemporal patterns of ongoing activity revealed by real-time optical imaging coupled with single-unit recording in the cat visual cortex. J Neurophysiol 73, 2072-93 (1995).

Berry, M. J., 2nd, Brivanlou, I. H., Jordan, T. A. & Meister, M. Anticipation of moving stimuli by the retina. Nature 398, 334-8 (1999).

Bullier, J. Integrated model of visual processing. Brain Res Brain Res Rev 36, 96-107 (2001).

Cantone, G., Xiao, J. & Levitt, J. B. Retinotopic organization of ferret suprasylvian cortex. Vis Neurosci 23, 61-77 (2006).

Cohen, L. B., Salzberg, B. M., Davila, H. V., Ross, W. N., Landowne, D., Waggoner, A. S. & Wang, C. H. Changes in axon fluorescence during activity: molecular probes of membrane potential. J Membr Biol 19, 1-36 (1974).

Diamond, I. T., Conley, M., Itoh, K. & Fitzpatrick, D. Laminar organization of geniculocortical projections in Galago senegalensis and Aotus trivirgatus. J Comp Neurol 242, 584-610 (1985).

Erikkson, D. & Roland, P. E. Feed-forward, feedback and lateral interactions in membrane potentials and spike trains from the visual cortex in vivo. J Physiol Paris 100, 100-9 (2006).

Felleman, D. J. & Van Essen, D. C. Distributed hierarchical processing in the primate cerebral cortex. Cereb Cortex 1, 1-47 (1991).

Gattass, R., Rosa, M. G., Sousa, A. P., Pinon, M. C., Fiorani Junior, M. & Neuenschwander, S. Cortical streams of visual information processing in primates. Braz J Med Biol Res 23, 375-93 (1990).

Geisler, W. S. Motion streaks provide a spatial code for motion direction. Nature 400, 65-9 (1999).

Grinvald, A., Hildesheim, R., Farber, I. C. & Anglister, L. Improved fluorescent probes for the measurement of rapid changes in membrane potential. Biophys J 39, 301-8 (1982).

Grinvald, A., Lieke, E. E., Frostig, R. D. & Hildesheim, R. Cortical point-spread function and long-range lateral interactions revealed by real-time optical imaging of macaque monkey primary visual cortex. J Neurosci 14, 2545-68 (1994).

Grinvald, A. & Hildesheim, R. VSDI: a new era in functional imaging of cortical dynamics. Nat Rev Neurosci 5, 874-85 (2004).

Hendrickson, A. E., Wilson, J. R. & Ogren, M. P. The neuroanatomical organization of pathways between the dorsal lateral geniculate nucleus and visual cortex in Old World and New World primates. J Comp Neurol 182, 123-36 (1978).

Hubel, D. H. & Wiesel, T. N. Receptive fields of single neurones in the cat's striate cortex. J Physiol 148, 574-91 (1959).

Hubel, D. H. & Wiesel, T. N. Receptive fields, binocular interaction and functional architecture in the cat's visual cortex. J Physiol 160, 106-54 (1962).

Jancke, D. Orientation formed by a spot's trajectory: a two-dimensional population approach in primary visual cortex. J Neurosci 20, RC86 (2000).

Jancke, D., Erlhagen, W., Schoner, G. & Dinse, H. R. Shorter latencies for motion trajectories than for flashes in population responses of cat primary visual cortex. J Physiol 556, 971-82 (2004).

Jones, J.P. & Palmer, L.A. An evaluation of the two-dimensional Gabor filter model of simple receptive fields in cat striate cortex. J Neurophysiol 58, 1233-58 (1987).

Khayat, P. S., Saint-Amour, D., Molotchnikoff, S., Lepore, F. & Guillemot, J. P. Cellular response to texture and form defined by motion in area 19 of the cat. Eur J Neurosci 12, 1727-38 (2000).

Lamme, V. A. & Roelfsema, P. R. The distinct modes of vision offered by feedforward and recurrent processing. Trends Neurosci 23, 571-9 (2000).

Livingstone, M. & Hubel, D. Segregation of form, color, movement, and depth: anatomy, physiology, and perception. Science 240, 740-9 (1988).

Lund, J. S. Anatomical organization of macaque monkey striate visual cortex. Annu Rev Neurosci 11, 253-88 (1988).

Manger, P. R., Kiper, D., Masiello, I., Murillo, L., Tettoni, L., Hunyadi, Z. & Innocenti, G.M. The representation of the visual field in three extrastriate areas of the ferret (Mustela putorius) and the relationship of retinotopy and field boundaries to callosal connectivity. Cereb Cortex 12, 423-37 (2002).

Manger, P. R., Masiello, I. & Innocenti, G. M. Areal organization of the posterior parietal cortex of the ferret (Mustela putorius). Cereb Cortex 12, 1280-97 (2002).

Manger, P. R., Nakamura, H., Valentiniene, S. & Innocenti, G. M. Visual areas in the lateral temporal cortex of the ferret (Mustela putorius). Cereb Cortex 14, 676-89 (2004).

Maunsell, J. H. & van Essen, D. C. The connections of the middle temporal visual area (MT) and their relationship to a cortical hierarchy in the macaque monkey. J Neurosci 3, 2563-86 (1983).

McIlwain, J. T. An Introduction to the Biology of Vision. Cambridge University Press (1996).

Mountcastle, V. B. Modality and topographic properties of single neurons of cat's somatic sensory cortex. J Neurophysiol 20, 408-34 (1957).

Ouellette, B. G. & Casanova, C. Overlapping visual response latency distributions in visual cortices and LP-pulvinar complex of the cat. Exp Brain Res 175, 332-41 (2006).

Palmer, S. E. Vision Sciencce. Photons to Phenomenology. MIT Press (2002).

Payne, B. R. Evidence for visual cortical area homologs in cat and macaque monkey. Cereb Cortex 3, 1-25 (1993).

Philipp, R., Distler, C. & Hoffmann, K. P. A motion-sensitive area in ferret extrastriate visual cortex: an analysis in pigmented and albino animals. Cereb Cortex 16, 779-90 (2006).

Roland, P. E. Dynamic depolarization fields in the cerebral cortex. Trends Neurosci 25, 183-90 (2002).

Roland, P. E., Hanazawa, A., Undeman, C., Eriksson, D., Tompa, T., Nakamura, H. & Valentiniene, S. Cortical feedback depolarization waves: a mechanism of top-down influence on early visual areas. Proc Natl Acad Sci U S A 103, 12586-91 (2006).

Schmidt, R. F., Thews, G. & Lang, F. Physiologie des Menschen. Springer-Verlag Berlin Heidelberg (2000).

Schroeder, C. E., Mehta, A. D. & Givre, S. J. A spatiotemporal profile of visual system activation revealed by current source density analysis in the awake macaque. Cereb Cortex 8, 575-92 (1998).

Shoham, D., Glaser, D. E., Arieli, A., Kenet, T., Wijnbergen, C., Toledo, Y., Hildesheim, R. & Grinvald, A. Imaging cortical dynamics at high spatial and temporal resolution with novel blue voltage-sensitive dyes. Neuron 24, 791-802 (1999).

Sincich, L. C. & Horton, J. C. The circuitry of V1 and V2: integration of color, form, and motion. Annu Rev Neurosci 28, 303-26 (2005).

Slovin, H., Arieli, A., Hildesheim, R. & Grinvald, A. Long-term voltage-sensitive dye imaging reveals cortical dynamics in behaving monkeys. J Neurophysiol 88, 3421-38 (2002).

Tasaki, I., Watanabe, A., Sandlin, R. & Carnay, L. Changes in fluorescence, turbidity, and birefringence associated with nerve excitation. Proc Natl Acad Sci U S A 61, 883-8 (1968).

Ungerleider, L. G., Galkin, T. W. & Mishkin, M. Visuotopic organization of projections from striate cortex to inferior and lateral pulvinar in rhesus monkey. J Comp Neurol 217, 137-57 (1983).

Ungerleider, L. G. & Haxby, J. V. 'What' and 'where' in the human brain. Curr Opin Neurobiol 4, 157-65 (1994).

Usrey, W. M., Sceniak, M. P. & Chapman, B. Receptive fields and response properties of neurons in layer four of ferret visual cortex. J Neurophysiol 89, 1003-15 (2003).

Waggoner, A. S. Dye indicators of membrane potential. Annu Rev Biophys Bioeng 8, 47-68 (1979).

Waggoner, A. S. & Grinvald, A. Mechanisms of rapid optical changes of potential sensitive dyes. Ann N Y Acad Sci 303, 217-41 (1977).

Zeki, S. M. Functional organization of a visual area in the posterior bank of the superior temporal sulcus of the rhesus monkey. J Physiol 236, 549-73 (1974).

8 Acknowledgements

Finally I would like to thank all the people that contributed to this project:

My supervisor, Prof. Dr. K. Amunts, for giving me the opportunity to start a research project at Karolinska Institutet, despite the distance to my home university. I am grateful for her support since the day I started my work.

Prof. Per E. Roland, MD, PhD, for supervising me in his lab, for his help with the experiments and data processing. And for the regular discussions of my project and this manuscript during and after my time at Karolinska.

David Eriksson, MSc, Tamas Tompa, PhD, and Michael Harvey, PhD, for their help with the experiments.

Calle Undemann, MSc, for writing all the programs I needed for data analysis, including my very own Sarah-button.

Sonata Valentiniene, MSc, for her great help with histology and animal handling.

Jesper Fredriksson, MSc, for introducing me into the beauty of matlab and for our many discussions.

Lars Forsberg, MSc, for keeping everybody updated on hard- and software.

Adolfo Talpalar, PhD, Alexander Walter, MSc, Shirin Ilkanizadeh, MSc, Kylie Foo, MSc, for their friendship and support.

Ahmet Bozkurt, MD, for finding time to support me, even in the busiest moments.

Thomas Erger for his support and help with programming and editing outside the walls of Karolinska.

My family for being my backup, for supporting all my steps and for their interest in my work and life way out North.

I owe special gratitute to the The Bohringer Ingelheim Foundation for supporting my work with a scholarship.

9 Erklärung zur Datenaufbewahrung

Hiermit erkläre ich, dass die dieser Dissertation zu Grunde liegenden Originaldaten bei meinem Co-Betreuer, Prof. Per E. Roland, MD, PhD, Institut für Neurowissenschaft des Karolinska Institutes Stockholm, Schweden, hinterlegt sind.

10 Curriculum Vitae

Last name:	Wehner
First name:	Sarah

Date of birth:	1984-04-26
Place of birth:	Aachen

Address:	Mühlenstraße 104
	52134 Herzogenrath
	Germany
Email	sarah.wehner@rwth-aachen.de

Education:	1990-1994	Primary school Herzogenrath, Germany
	1994-2002	Grammar school Würselen, Germany
University:	since 2002	Medical school RWTH Aachen University, Germany
	2004	Preliminary medical examination (Physikum)
	2005-2006	Dissertation project in Per Rolands's group at the Institute of Neuroscience, Division of Brain Research, Karolinska Institutet, Stockholm, Sweden
	2008	Clinical electives: a) Akademiska Sjukhuset, Uppsala, Sweden b) Luisenhospital Aachen, Germany c) Mayo General Hospital, Castlebar, Ireland
	2009-05-19	State Examination